**UNIVERSITY OF GAZİANTEP**

**GRADUATE SCHOOL OF**

**NATURAL & APPLIED SCIENCES**

# STATE FEEDBACK CONTROL OF UNDERACTUATED MANIPULATORS

**M. Sc. THESIS**

**IN**

**ELECTRICAL-ELECTRONICS ENGINEERING**

**BY**

**MEHMET ARICI**

**AUGUST 2013**

# State Feedback Control of Underactuated Manipulators

**M.Sc. Thesis**

**in**

**Electrical-Electronics Engineering**

**University of Gaziantep**

**Supervisor**
**Assist. Prof. Dr. Tolgay KARA**

**by**

**Mehmet ARICI**

**August 2013**

REPUBLIC OF TURKEY

UNIVERSITY OF GAZİANTEP
GRADUATE SCHOOL OF NATURAL & APPLIED SCIENCES
ELECTRICAL – ELECTRONICS ENGINEERING

Name of the thesis: State Feedback Control of Underactuated Manipulators

Name of the student: Mehmet ARICI

Exam date: 01.08.2013

Approval of the Graduate School of Natural and Applied Sciences

Assoc.Prof.Dr. Metin BEDİR

Director

I certify that this thesis satisfies all the requirements as a thesis for the degree of Master of Science.

Prof. Dr. Celal KORAŞLI

Head of Department

This is to certify that we have read this thesis and that in our consensus opinion it is fully adequate, in scope and quality, as a thesis for the degree of Master of Science.

Asst. Prof. Dr. Tolgay KARA

Supervisor

Examining Committee Members

Prof. Dr. L. Canan DÜLGER .....

Prof. Dr. Ergun ERÇELEBİ .....

Assist. Prof. Dr. Tolgay KARA .....

**I hereby declare that all information in this document has been obtained and presented in accordance with academic rules and ethical conduct. I also declare that, as required by these rules and conduct, I have fully cited and referenced all material and results that are not original to this work.**

Mehmet ARICI

## ABSTRACT

### STATE FEEDBACK CONTROL OF UNDERACTUATED MANIPULATORS

ARICI, Mehmet

M.Sc. in Electrical-Electronics Engineering

Supervisor: Assist. Prof. Dr. Tolgay KARA

August 2013, 60 pages

Underactuated manipulators are widely used in robotic and mechatronic applications. Control of underactuated mechanical systems is difficult since they have fewer control inputs (actuators) than degrees of freedom. This thesis considers a two-degree-of-freedom manipulator with one active joint at shoulder and moves on horizontal plane. Controlling the manipulator in horizontal plane is another challenging work since the gravity has no effect on free joint of manipulator.

To solve the control problem a nonlinear state feedback controller is developed. Partial feedback linearization technique is used for controlling each joint angle position and in order to control both joints simultaneously a switching control algorithm is adopted to the control system.

Designed control system is applied to the manipulator in simulations and for various initial conditions, controlled system performance is observed. Furthermore, the same controller is implemented to real-time prototype of manipulator and applicability of controller to a real system is tested. In both simulation and real-time implementation satisfactory results are obtained. Proposed control system moves the manipulator links to desired positions in a short time interval and input torque needed is small enough to apply the controller to a real system. Results also show that we achieve position control objective with small steady-state errors which are in an acceptable range.



**Key Words**: State feedback control, switching control, underactuted manipulators, partial feedback linearization, computed torque control, real-time control applications

# ÖZET

## EKSİK TAHRİKLİ MANİPÜLATÖRLERİN DURUM GERİ BESLEMELİ KONTROLÜ

ARICI, Mehmet

Yüksek Lisans Tezi, Elektrik-Elektronik Mühendisliği Bölümü

Tez Yöneticisi: Yrd. Doç. Dr. Tolgay KARA

Ağustos 2013, 60 sayfa

Eksik tahrikli manipülatörler, mekatronik ve robotik uygulamalarında fazlaca kullanılmaktadır. Eksik tahrikli manipülatörlerin kontrolü, sistemin tahrik elemanı (kontrol giriş) sayısının sistem serbestlik derecesinden az olduğu için zor bir hal almaktadır. Bu tezde, iki serbestlik dereceli, ilk mafsalda tahrik elemanı bulunduran ve yatay düzlemde çalışan bir manipülatör ele alınmıştır. Yatay düzlemde serbest dönebilen ekleme yer çekimi etki etmediğinden bu koşulda manipülatörü kontrol etmek daha zor hale gelmektedir.

Pozisyon kontrolü problemini çözmek için doğrusal olmayan durum geri beslemeli kontrol sistemi geliştirilmiştir. Kısmi geri beslemeli doğrusallaştırma tekniğiyle manipülatörün her bir ekleminin pozisyonunu kontrol etmek için kullanılmış ve her iki mafsalı aynı anda kontrol etmek amacıyla anahtarlamalı kontrol algoritması kontrol sistemine dahil edilmiştir. Tasarlanan kontrol sisteminin performansı simülasyonlarla ve gerçek zamanlı çalışan bir prototip yardımıyla test edilmiş; hem simülasyonlarda hem de gerçek zamanlı kontrol uygulamarında tatminkar sonuçlar elde edilmiştir. Önerilen kontrol sistemi manipülatörün mafsallarını istenilen pozisyonlara kısa sürede götürmüş ve uygulanan torkun gerçek sistemlerde kullanılabilir düzeyde olduğu görülmüştür. Sonuçlar pozisyon kontrol hedefine sürekli rejimde kabul edilebilir derecede küçük hatalarla varıldığını göstermektedir.



**Anahtar Kelimeler :** Durum geri beslemeli kontrol, anahtarlamalı kontrol, eksik tahrikli manipülatörler, kısmi geri besleme doğrusallaştırma, hesaplanan tork kontrol, gerçek zamanlı kontrol uygulamaları.

*"To my family"*

## ACKNOWLEDGEMENTS

I would like to express my deepest gratitude to my supervisor Asst. Prof. Dr. Tolgay KARA for his guidance, advice, criticism, encouragements and insight throughout this study.

I would like to thank to colleagues, Mehmet DEMİR, Ali Osman ARSLAN and Mahmut AYKAÇ for supporting and encouraging me with their best wishes.

Special thanks to my friend Seydi KAÇMAZ for his kind help and encouragement.

Finally, I would like to deeply thank my mother, father and my family for their love and emotional support.

## TABLE OF CONTENTS

## LIST OF FIGURES

## LIST OF TABLES

## LIST OF SYMBOLS/ABBREVIATIONS

| | |
|---|---|
| LQR | Linear Quadratic Regulator |
| DOF | Degree of Freedom |
| PD | Proportional Derivative |
| EMF | Electromotive Force |
| ppr | Pulse Per Revolution |
| ADC | Analog-to-digital Converter |
| DAC | Digital-to-analog Converter |
| ICM | Input Capture Module |
| OCM | Output Compare Module |
| QEM | Quadrature-encoder Module |
| PWM | Pulse-width Modulator |
| UART | Universal-asynchronous-receiver-transmitter |

# CHAPTER I

# INTRODUCTION

Recently, a lot of attention has been given to the control of mechanical systems where the number of control inputs are less than that of degrees of freedom or generalized coordinates. Such mechanical systems are said to be underactuated systems. Mechanical systems may become underactuated because of failure of one or more actuators. Underactuated systems can also appear in the mathematical model used for control design such as the joint or link flexibility is included in the model. These systems exist in a broad range of applications including robotics, aerospace systems, marine systems, flexible systems mobile systems and locomotive systems. Pendubot, acrobot, planar underactuated manipulator, inverted pendulum, double inverted pendulum, gymnast robot, cart pendulum, inverted wedge are typical examples of undeactuated systems.

## 1.1. Motivation

The underactuated robots have many advantages, such as light weight, low energy consumption, high security, self-fault tolerance they have and so on. Especially in the area of astronautics, it has a great application prospect, as the payload sent into the outer space is very expensive, the manipulators of the space robots can be made by extremely light and high strength carbon fiber material, but at present, driving motor can not be made very light, and using the underactuated joints not only can reduce the weight of the space robots, but also can enhance the flexibility of the system. The underactuated systems also arise naturally when trying to develop controllers for spacecraft, satellites and hovercraft and as popular laboratory test examples such as the inverted pendulum cart, the ball and beam, and the inertia wheel pendulum. Since underactuated mechanical systems are so broad and have complicated variant dynamics, many research efforts have been made on control aspects and strategies of underactuated systems.

Control of underactuated manipulators with passive joints operating in the horizontal plane is a special challenge. This underactuated mechanical system has been subject

of extensive research to develop various control algorithms to deal with the complication of the nonlinearity, instability, and controllability of the underactuated system. Since the dynamics of the manipulator is not affected by gravitational terms are a linearization about an equilibrium point leads to a linear system which is not controllable. The system also has second order nonholonomic constraints which are not integrable. It is thus clear that there is a need to develop control techniques applicable to this kind of systems. To investigate the control problem, a two link planar manipulator arm which has a free joint and operates in the horizontal plane is considered in this thesis.

### 1.2. Literature Review

Several authors proposed different control methods which are linear or nonlinear depending on physical and mechanical conditions of the underactuated manipulator. For instance, in the presence of gravity, underactuated manipulators can be linearized about some specific points although they are not fully linearizable. Most researchers have used linear control theory, in this case, to balance the systems about equilibrium points. Daniel Jerome [1] has used linear quadratic regulator (LQR) technique for balancing the Pendubot about the upright equilibrium point. Fantoni and Lozano [2] have used full state feedback linear controller for balancing the acrobot about the equilibrium position. G.Giua and A.Usai have developed a gain-scheduling controller for overhead cranes [3]. On the other hand, some researchers used nonlinear control for the same system. Spong and Praly [4] have presented the partial feedback linearization technique for swinging up underactuated robots about unstable equilibrium points. They have considered acrobot, which is a two link manipulator having one actuator at the elbow joint and the other one is completely free and three-link gymnast robot and cart pole system. Daniel Jerome [1] has designed two-link underactuated manipulator (Pendubot), and used partial feedback linearization technique for a swing up control and linear quadratic regulator (LQR) technique for balancing the manipulator about the upright equilibrium point. Isabelle Fantoni and Rogelio Lozano [2] have presented energy based approach for swinging up the Pendubot and used Lyapunov theory for convergence analysis. Also they have used full-state feedback linear controller for balancing the manipulator at the equilibrium position. In [5], K. L. Carroll presented a robust sliding mode controller for acrobot

while in [6] W. Wang and D. Liu have presented a sliding mode controller for overhead crane.

In the absence of gravity which means the manipulator operates in horizontal plane, control problem is more difficult. There are also a lot of studies that examine the system and suggest different control strategies. Arai and Tachi [7] have presented a method of controlling the position of an underactuated manipulator equipped with motors and encoders on active joints, and holding brakes and encoders on passive joints. The passive joints are excited to the desired position using dynamic decoupling and held on the desired position by engaging the holding brakes. Also Arai and Tachi [7] have described the controllability conditions of such manipulators. In [11], Arai has proved the controllability of a 3-DOF underactuated manipulator (that is not equipped with brakes on passive joints) by a constructive method in which the trajectory from any initial state to any desired state is composed. In [12], Marcel Bergerman have studied the controllability of planar manipulators and developed robust optimal sequential control methods for the underactuated manipulators using variable structure controllers with the aid of brakes on passive joints. He has also developed a graphical method to plan a collision–free motion of the manipulator inside its constrained configuration space. On the other side, Norbert Scherm and Bodo Heimann [13] have proposed a discrete time approach based on sensitivity functions for the same system. Tian Zhixiang [14] has presented a discontinuous control method which divides the system into active and passive subsystem and designed adaptive laws with bacstepping algorithm to control overall system.

### 1.3. Problem Statement and Contribution of Thesis

Position control problem of a two link underactuted manipulator which moves in horizontal plane and has two revolute joints is considered in this thesis. The manipulator is an example of a mechanical system with second-order nonholonomic constraints. In particular, the dynamic equation of the unactuated joints is a second-order constraint on generalized coordinates which is in general non-integrable. This is in contrast with the vast majority of literature on nonholonomic systems, where only first-order (kinematic) constraints have been presented. Furthermore, as we will see in following chapters, linearization of the system about any equilibrium point is

not controllable. It means that we can not control both joints of the manipulator simultaneously by using a linear state feedback control method. It must be emphasized that if the manipulator operated in vertical plane it would simplify the control problem, making the linearization around any equilibrium point controllable because of inclusion of gravity terms in the dynamic equation of the system. In this case even a linear controller will eventually stabilize the system. Consequently, linear stabilization tools cannot be used even locally. Moreover, there is a fundamental obstruction to existence of smooth time-invariant feedback laws. In the case of horizontal operating condition, system might be asymptotically stabilizable by means of nonlinear feedback. A number of approaches have been proposed for stabilization of nonholonomic control systems to an equilibrium. Approaches can be classified as discontinuous time-invariant stabilization, time varying stabilization and hybrid stabilization. For these reasons a nonlinear state feedback control law is proposed for an underactuated manipulator in thesis. Firstly, for each joint, a partly stable control law is designed by using partial feedback linearization technique and computed torque control method. Then, to control the overall system, a logic based switching rule which depends on energy-like error functions of the joint angles and velocities and chooses the suitable partly stable controller is used as a supervisor.

### 1.4. Organization of Thesis

The previous sections give an overview about underactuated systems and at which conditions this behavior occurs. Then some solutions of the control problem are given in previous studies. The mathematical model of the system and its properties are discussed further in Chapter II.

Chapter III presents control problem of the underactuated manipulator. A brief background of the proposed control methodologies and strategies are also given and then purposed control system is explained.

After control system is designed, simulation of the manipulator based on the designed controller is given Chapter IV and performance of the manipuator is tested by the simulated system. Chapter V give information about construction of real prototype system and performance of the controller on the prototype is also observed and results are given. In Chapter VI results and conclusions are generally discussed.

# CHAPTER II

# MATHEMATICAL MODEL OF 2-DOF UNDERACTUATED MANIPULATOR

## 2.1. Introduction

The first step in the controller design for two-link planar underactuated manipulator is to develop mathematical model for it. This task is achieved in the following sections.

In general, dynamic equations may be used to find the equations of motion of mechanisms. This means that knowing the forces and torques, one can figure out how a mechanism will move. The techniques such as Newtonian mechanics can be used to find the dynamic equations for robots. However, due to the fact that robots are three dimensional, multiple-degree-of-freedom mechanisms with distributed masses, it is very difficult to use Newtonian mechanics. Instead, one may choose to use other techniques such as Lagrangian mechanics. Lagrangian is based on energy terms only and thus in many cases is easier to use. Although Newtonian mechanics, as well as other techniques, can be used for this derivation, most of references are based on Lagrangian mechanics.

With Lagrange formulation, the equations of motion can be derived in a systematic way independently of the reference coordinate frame. Once a set of variables $q_i$ , $i$ =1, ……, $n$ termed as the generalized coordinates, are chosen which effectively describe the link positions of an n-DOF manipulator, the Lagrangian of the generalized coordinates:

$$L = K - P \tag{2.1}$$

where $K$ and $P$ respectively denote the total kinetic energy and potetial energy of the system. Then :

$$\frac{\partial}{\partial t}\left(\frac{\partial L}{\partial \dot{q}_i}(q,\dot{q})\right) - \frac{\partial L}{\partial q_i}(q,\dot{q}) = \tau_i \tag{2.2}$$

where τ is the sum of all torques in a rotational motion. States q and q̇ are joint angular positions and velocities respectively. As a result, to get the equations of motion, we need to derive energy equations for the system and then differentiate the Lagrangian according to equation (2.2).

### 2.2. Equations of Motion via Lagrange Formulation

First we calculate the kinetic and potential energies of the system for which the coordinate description is given in Figure 2.1 to obtain equations of motion with Lagrangian mechanics.

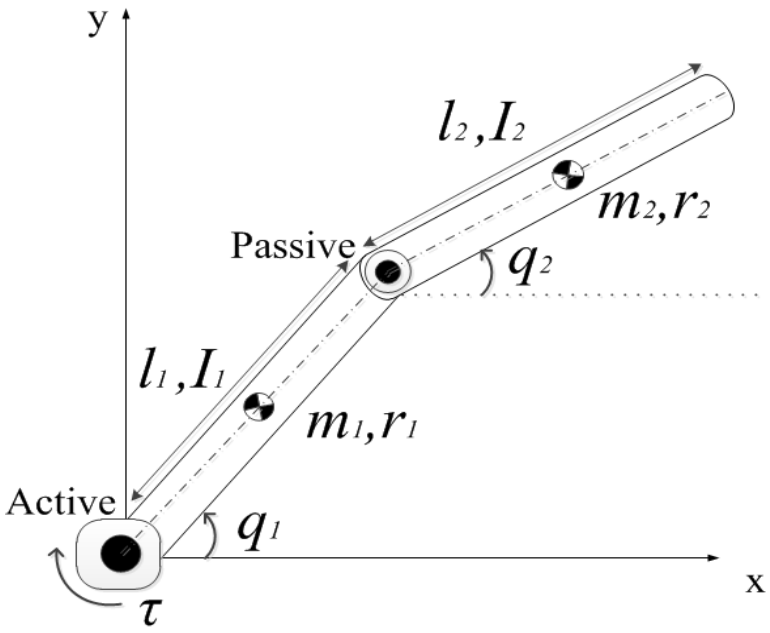


**Figure 2. 1.** Coordinate description of underactuated manipulator

Kinetic energy of the first link of the manipulator is given by :

$$K_1 = \frac{1}{2}(I_1 + m_1 r_1^2)\dot{q}_1^2 \tag{2.3}$$

Kinetic energy of the second link:

$$K_2 = \frac{1}{2}(I_2 + m_2 l_1 r_2 \cos q_2 + m_2 r_2^2 + m_2 l_1^2)\dot{q}_1^2 + (I_2 + m_2 l_1 r_2 \cos q_2 + m_2 r_2^2)\dot{q}_1\dot{q}_2 + \frac{1}{2}(I_2 + m_2 r_2^2)\dot{q}_2^2 \quad (2.4)$$

Total kinetic energy of the system is:

$$K = K_1 + K_2 \quad (2.5)$$

To simplify the equations we introduce three parameters $\theta_i$, i = (1, .., 3) in the following form:

$$\theta_1 = m_1 r_1^2 + m_2 l_1^2 + I_1 \quad (2.6)$$

$$\theta_2 = m_1 r_2^2 + I_2 \quad (2.7)$$

$$\theta_3 = m_2 l_1 r_2 \quad (2.8)$$

By using the parameters introduced total kinetic energy can be written in the following form:

$$K = \frac{1}{2}(\theta_1 + \theta_2 + 2\theta_3 \cos q_2)\dot{q}_1^2 + \frac{1}{2}\theta_2\dot{q}_2^2 + (\theta_2 + \theta_3 \cos q_2)\dot{q}_1\dot{q}_2 \quad (2.9)$$

Potential energy of the system is also sum of the energies of the two links. This energy is only depends on the position of each joint. However, since we assume that the manipulator moves in horizontal plane we can cancel the terms which contain gravity. In this case, total potential energy of the manipulator is zero and Lagrangian function takes the following form:

$$L = \frac{1}{2}(\theta_1 + \theta_2 + 2\theta_3 \cos q_2)\dot{q}_1^2 + \frac{1}{2}\theta_2 \dot{q}_2^2 + (\theta_2 + \theta_3 \cos q_2)\dot{q}_1\dot{q}_2 \quad (2.10)$$

In order to find elements of Lagrange equation given in (2.2), Lagrange function above is used. Following equations give these elements :

$$(\frac{\partial L}{\partial \dot{q}_1}) = (\theta_1 + \theta_2 + 2\theta_3 \cos q_2)\dot{q}_1 + (\theta_2 + \theta_3 \cos q_2)\dot{q}_2 \quad (2.11)$$

$$(\frac{\partial L}{\partial q_1}) = 0 \quad (2.12)$$

$$(\frac{\partial L}{\partial \dot{q}_2}) = (\theta_2 + \theta_3 \cos q_2)\dot{q}_1 + \theta_2 \dot{q}_2 \quad (2.13)$$

$$(\frac{\partial L}{\partial q_2}) = -\theta_3 \sin q_2 \dot{q}_1^2 - \theta_3 \sin \dot{q}_1\dot{q}_2 \quad (2.14)$$

where $q = (q_1, q_2)^T$ is joint positions vector and $\tau = (\tau_1, 0)^T$ is actuation torque of the joints. In our case only shoulder joint is actuated and there is no actuation in the elbow joint. From Lagrangian derivations the dynamic equations of the manipulator are obtained as given below:

$$\begin{aligned}&(\theta_1 + \theta_2 + 2\theta_3 \cos q_2)\ddot{q}_1 + (\theta_1 + \theta_3 \cos q_2)\ddot{q}_2 - \theta_3 \sin(q_2)\dot{q}_2^2 \\ &-2\theta_3 \sin(q_2)\dot{q}_1\dot{q}_2 = \tau_1\end{aligned} \quad (2.15)$$

$$\theta_2 \ddot{q}_2 + (\theta_2 + \theta_3 \cos q_2)\ddot{q}_1 + \theta_3 \sin(q_2)\dot{q}_1^2 = 0 \quad (2.16)$$

The equation of motion can be written in the compact matrix form which represents the joint space dynamics as :

$$M(q)\ddot{q} + H(q, \dot{q}) = \tau \quad (2.17)$$

where

$M(q)$ : Symmetric positive definite inertia matrix

$H(q, \dot{q})$ : Centipetal and coriolis term matrix

$\tau$ : Joint torques

If we rewrite equations (2.15) and (2.16) in the compact form given in (2.17), inertia matrix, coriolis matrix and joint torque matrix for the manipulator we considered are as given below:

$$q = \begin{bmatrix} q_1 & q_2 \end{bmatrix}^T$$

$$\tau = \begin{bmatrix} \tau_1 & 0 \end{bmatrix}^T$$

$$M(q) = \begin{bmatrix} \theta_1 + \theta_2 + 2\theta_3 \cos q_2 & \theta_2 + \theta_3 \cos q_2 \\ \theta_2 + \theta_3 \cos q_2 & \theta_2 \end{bmatrix}$$

$$H(q, \dot{q}) = \begin{bmatrix} -\theta_3 \sin q_2 (2\dot{q}_1 \dot{q}_2 + \dot{q}_2^2) \\ \theta_3 \sin(q_2) \dot{q}_1^2 \end{bmatrix}$$

In the manipulator dynamic equation, a coefficient in the form of $M_{11}$ is known as effective inertia at joint1, such that an acceleration at joint1 causes a torque at joint1 equal to $M_{11}\ddot{q}_1$, whereas a coefficient in the form $M_{12}$ is known as coupling inertia between first and second joints as an acceleration at joint1 or joint2 causes a torque at joint1 or joint2 equal to $M_{12}\ddot{q}_1$. All terms with $\dot{q}_1\dot{q}_2$ represent coriolis accelerations and when multiplied by corresponding inertias they will represent coriolis forces. Remaining terms which contain quadratic velocities of joints like $\dot{q}_1^2$ and $\dot{q}_2^2$ represents centripetal forces acting on related joint due to a velocity at other joint.

If we regard the nonconservative forces doing work at the manipulator joints, those are given by actuation torques $\tau$ minus the viscous friction torques and the static friction torques general formulation of the system takes the following form:

$$M(q)\ddot{q} + H(q, \dot{q}) + F_v \dot{q} + F_s \, sgn(\dot{q}) = \tau \qquad (2.18)$$

where $F_v$ denotes the 2x2 diagonal matrix of viscous friction coefficients, and $F_s$ is a 2x2 diagonal matrix of static friction coefficients.

### 2.3. The State Space Based Description

Because the matrix M(q) is positive definite, the inverse matrix of it, $M(q)^{-1}$, exists. The system motion equation can then be written as:

$$\ddot{q} = M(q)^{-1}(\tau - H(q,\dot{q})) \tag{2.19}$$

If we define the state vector x as follows :

x : $x_1 = q_1$, $x_2 = \dot{q}_1$, $x_3 = q_2$, $x_4 = \dot{q}_2$

The state space description of the system can be obtained as follows:

$$\dot{x} = f(x) + g(x)u \tag{2.20}$$

where

$$f_1(x) = x_2$$

$$f_2(x) = \frac{\theta_2\theta_3(x_1 + x_4)^2 \sin x_3 + \theta_3 x_2^2 \sin x_3 \cos x_3}{\theta_1\theta_2 - \theta_3 \cos^2 x_3}$$

$$f_3(x) = x_4$$

$$f_4(x) = -f_2(x) - \frac{\theta_3^2(x_2 + x_4)^2 \sin x_3 \cos x_3 + \theta_1\theta_3 x_2^2 \sin x_3}{\theta_1\theta_2 - \theta_3^2 \cos^2 x_3}$$

$$g_1(x) = 0$$

$$g_2(x) = \frac{\theta_2}{\theta_1\theta_2 - \theta_3^2 \cos^2 x_3}$$

$$g_3(x) = 0$$

$$g_4(x) = -\frac{\theta_2 + \theta_3 \cos x_3}{\theta_1\theta_2 - \theta_3^2 \cos^2 x_3} \tag{2.21}$$

Parameters $\theta_1$ to $\theta_3$ above are defined in equations (2.6), (2.7) and (2.8), u is the input torque applied to the shoulder motor, and $x_1$ to $x_4$ are state variables of the manipulator.

### 2.4. The Equilibrium Manifold

Underactuated mechanical systems generally have equilibria which depend on both their kinematic and dynamic parameters. If the underactuated manipulator is mounted so that the joint axes are parallel to gravity, then there will be a continuum of equilibrium configurations exist only when the input torque is zero. In some other researches on the planar robot, the joint axes of the system are set to be perpendicular to the gravity in which case the continuum of equilibrium configurations exists, each corresponding to a constant value, $\bar{\tau}$, of the input torque $\tau$ [15, 16].

If $(q, \dot{q}) = (q^e, 0)$ is an equilibrium solution for the system, $q^e$ is referred to as an equilibrium configuration. For the manipulator dynamics, the equilibrium configuration is given by $\{q \in Q : M(q)^{-1}H(q, 0) = 0\}$. It is thus clear that all points $q \in Q$ are equilibrium configurations. The control object is to move the links from rest to a target-configuration with zero-velocity.

# CHAPTER III

# CONTROL METHOD

As mentioned before, because of horizontal operating condition, linearization of underactuated system considered in the thesis in not controllable. The system also has very complicated nonlinear structure and nonholonomic constraints. All these properties of the manipulator still make its control issue an open problem as given in the literature review. As a matter of fact, manipulators with passive joints in the absence of gravity cannot be stabilized at a point by smooth static feedback, as they violate the condition due to Brocket [17]. As a consequence, any feedback law solving the position control problem of the manipulator must necessarily be discontinuous and/or time-varying.

In this thesis, to solve the control problem a discontinuous nonlinear state feedback controller is proposed. Partial feedback linearization and computed torque control is used to design partly stable state feedback controllers for each link of manipulator. These controllers can stabilize only the related joint that linearization process is applied. Then, in order to design a supervisory switching controller that stabilizes the whole system, an energy like error function is given such that it includes position and velocity errors of joints according to desired and actual values of the state variables.

## 3.1. Controllability of Underactuated Manipulator

In the horizontal plane, the components of potential energy are not included as mentioned in the previous chapter. Thus, the equations of motion for the underactuated manipulator in the horizontal plane, are as it is expressed in the equations (2.15) and (2.16).

Let us rewrite equations (2.15) and (2.16) in the following manner :

$$\ddot{q}_1 = \frac{1}{\theta_1\theta_2 - \theta_3^2 \cos^2 q_2}\left[\theta_2\theta_3 \sin q_2(\dot{q}_1 + \dot{q}_2)^2 + \theta_3^2 \cos q_2 \sin(q_2)\dot{q}_1^2 + \theta_2\tau_1\right] \tag{3.1}$$

$$\ddot{q}_2 = \frac{1}{\theta_1\theta_2 - \theta_3^2 \cos^2 q_2}\begin{bmatrix} -\theta_3(\theta_2 + \theta_3 \cos q_2)\sin q_2(\dot{q}_1 + \dot{q}_2)^2 - (\theta_1 + \theta_3 \cos q_2)\sin(q_2)\dot{q}_1^2 \\ -(\theta_2 + \theta_3 \cos q_2)\tau_1 \end{bmatrix} \tag{3.2}$$

Differentiating equations (3.1) and (3.2) with respect to the states $[x_1 = q_1,\ x_2 = \dot{q}_1, x_3 = q_2,\ x_4 = \dot{q}_2]$and evaluating them at arbitrary position $[\theta_1 = \theta_{ar1},\ \dot{\theta}_1 = 0, \theta_2 = \theta_{ar2},\ \dot{\theta}_2 = 0]$, reveals the following state space equation:

$$\dot{x} = Ax + Bu \tag{3.3}$$

where

$$\dot{\mathbf{x}} = \begin{bmatrix} 0 & 1 & 0 & 0 \\ 0 & 0 & 0 & 0 \\ 0 & 0 & 0 & 1 \\ 0 & 0 & 0 & 0 \end{bmatrix} x + \begin{bmatrix} 0 \\ N_1 \\ 0 \\ N_2 \end{bmatrix} \tag{3.4}$$

The terms $N_1$ and $N_2$ are constants resulted from evaluating the partial differential equation at arbitrary positions $[\theta_1 = \theta_{ar1}, \theta_2 = \theta_{ar2}]$.

$$N_1 = \frac{\theta_2}{\theta_1\theta_2 - \theta_3^2 \cos^2 q_2}, N_2 = -\frac{\theta_2 + \theta_3 \cos q_2}{\theta_1\theta_2 - \theta_3^2 \cos^2 q_2}$$

Therefore

$$\mathbf{A} = \begin{bmatrix} 0 & 1 & 0 & 0 \\ 0 & 0 & 0 & 0 \\ 0 & 0 & 0 & 1 \\ 0 & 0 & 0 & 0 \end{bmatrix} \quad \mathbf{B} = \begin{bmatrix} 0 \\ N_1 \\ 0 \\ N_2 \end{bmatrix} \quad AB = \begin{bmatrix} N_1 \\ 0 \\ N_2 \\ 0 \end{bmatrix} \quad A^2B = \begin{bmatrix} 0 \\ 0 \\ 0 \\ 0 \end{bmatrix} \quad A^3B = \begin{bmatrix} 0 \\ 0 \\ 0 \\ 0 \end{bmatrix}$$

And

$$\begin{bmatrix} B & AB & A^2B & A^3B \end{bmatrix} = \begin{bmatrix} 0 & N_1 & 0 & 0 \\ N_1 & 0 & 0 & 0 \\ 0 & N_2 & 0 & 0 \\ N_2 & 0 & 0 & 0 \end{bmatrix}$$

It is clear that the matrix $[B \quad AB \quad A^2B \quad A^3B]$ which determines the controllability of the system is singular (rank=2<4). Thus, as in [18] the two link manipulator is uncontrollable in the absence of gravity terms and friction terms. Therefore positioning the underactuated manipulator at desired position is done with aid of holding brakes in some previous researches.

### 3.2. Computed-Torque Control

Computed-torque control gives one the ability to obtain a linear version of a nonlinear system by means of the state variables. The equation of motion (2.17) that exhibits charactersitic behaviour of robot manipulator, generally comprises nonlinear functions of state variables (joint positions and velocities). A controller can be compesed of nonlinear functions of the state variables in the closed-loop form but it can also be described by a linear differential equation. This controller is capable of fulfilling the motion control objective, globally and moreover with a trivial selection of its design parameters.

The computed-torque control law is given as follows :

$$\tau = M(q)\left[\ddot{q}_d + K_V\dot{\tilde{q}} + K_P\tilde{q}\right] + H(q,\dot{q}) \tag{3.5}$$

Where $K_V$ and $K_P$ are symmetric positive definite design matrices and $\tilde{q} = q_d - q$ generally denotes the position error.

Control law (3.5) contains the terms $K_V\dot{\tilde{q}} + K_P\tilde{q}$ which are of PD type. However, these terms are actually multiplied by the inertia matrix $M(q_d - \tilde{q})$. Therefore this is not a linear controller as the PD, since the position and velocity gains are not constant but they depend explicitly on the position error $\tilde{q}$. This may be clearly seen when expressing the computed-torque control law given by (3.5) as :

$$\tau = M(q_d - \tilde{q})K_P\tilde{q} + M(q_d - \tilde{q})K_V\dot{\tilde{q}} + M(q)\ddot{q} + H(q,\dot{q}) \tag{3.6}$$

The closed-loop equation is obtained by substituting the control action τ from (3.5) in the equation of manipulator model (2.17) to obtain

$$M(q)\ddot{q} = M(q)\left[\ddot{q}_d + K_V\dot{\tilde{q}} + K_P\tilde{q}\right] + H(q,\dot{q}) \tag{3.7}$$

Since M(q) is a positive definite matrix, we can apply inverse matrix operation and equation (3.7) reduces to

$$\ddot{q}_d + K_V\dot{\tilde{q}} + K_P\tilde{q} = 0 \tag{3.8}$$

which in turn may be expressed in terms of the state vector $\left[\tilde{q}^T + \dot{\tilde{q}}^T\right]^T$ as :

$$\frac{d}{dt}\begin{bmatrix}\tilde{q}\\ \dot{\tilde{q}}\end{bmatrix} = \begin{bmatrix}0 & I\\ -K_P & -K_V\end{bmatrix}\begin{bmatrix}\tilde{q}\\ \dot{\tilde{q}}\end{bmatrix} \tag{3.9}$$

where I is the identity matrix of dimension n.

It is important to point out that the closed loop equation (3.9) is represented by a linear autonomous differential equation, which unique equilibrium point is given by $\left[\tilde{q}^T + \dot{\tilde{q}}^T\right]^T = 0 \in \mathbb{R}^{2n}$. This single equilibrium point in the origin since the matrix $K_P$ is designed to be positive definite and therefore nonsingular.

Since the closed-loop equation (3.9) is linear and autonomous, its solutions may be obtained in closed form and be used to conclude about the stability of the origin. This can be done by using Lyapunov's direct method.

To that end, we start by introducing the constant ε satisfying

$$\lambda_{min}\{K_V\} > \varepsilon > 0$$

Multiplying by $x^Tx$ where $x \in \mathbb{R}^n$ is any nonzero vector, we obtain :

$$\lambda_{min}\{K_V\}\,x^Tx > \varepsilon x^Tx$$

Since $K_V$ is by design, a symmetric matrix then :

$$x^TK_Vx \geq \lambda_{min}\{K_V\}\,x^Tx$$

and therefore,

$$x^T \left[K_V - \varepsilon I\right] x > 0 \qquad \forall x \neq 0 \in \mathbb{R}^n$$

This means that the matrix $K_v - \varepsilon I$ is positive definite, i.e.

$$K_v - \varepsilon I > 0 \tag{3.10}$$

Considering all this, the positivity of the matrix $K_P$ and constant $\varepsilon$ we can conclude that

$$K_P + \varepsilon K_v - \varepsilon^2 I > 0 \tag{3.11}$$

If a Lyapunov function candidate is chosen as

$$V(\tilde{q}, \dot{\tilde{q}}) = \frac{1}{2}\begin{bmatrix}\tilde{q} \\ \dot{\tilde{q}}\end{bmatrix}^T \begin{bmatrix}K_p + \varepsilon K_V & \varepsilon I \\ \varepsilon I & I\end{bmatrix}\begin{bmatrix}\tilde{q} \\ \dot{\tilde{q}}\end{bmatrix}$$

$$V(\tilde{q}, \dot{\tilde{q}}) = \frac{1}{2}\dot{\tilde{q}}^T\dot{\tilde{q}} + \frac{1}{2}\tilde{q}^T\left[K_P + \varepsilon K_v\right]\tilde{q} + \varepsilon\tilde{q}^T\dot{\tilde{q}} \tag{3.12}$$

Evaluating the total time derivative of $V(\tilde{q}, \dot{\tilde{q}})$ we get :

$$V(\tilde{q}, \dot{\tilde{q}}) = \frac{1}{2}\ddot{\tilde{q}}^T\dot{\tilde{q}} + \frac{1}{2}\tilde{q}^T\left[K_P + \varepsilon K_v\right]\dot{\tilde{q}} + \varepsilon\dot{\tilde{q}}^T\dot{\tilde{q}} + \varepsilon\tilde{q}^T\ddot{\tilde{q}} \tag{3.13}$$

Substituting $\ddot{\tilde{q}}$ from the closed-loop equation (3.9) in the previous expression and after simplifying it, we obtain

$$V(\tilde{q}, \dot{\tilde{q}}) = -\begin{bmatrix}\tilde{q} \\ \dot{\tilde{q}}\end{bmatrix}^T \begin{bmatrix}\varepsilon K_P & 0 \\ 0 & K_V - \varepsilon I\end{bmatrix}\begin{bmatrix}\tilde{q} \\ \dot{\tilde{q}}\end{bmatrix} \tag{3.14}$$

Now, since $\varepsilon$ is chosen so that $K_V$-$\varepsilon I > 0$, and since $K_P$ is by design positive definite, the function $V(\tilde{q}, \dot{\tilde{q}})$ in equation (3.14) is globally negative definite. In this case the

origin $\left[\tilde{q}^T + \dot{\tilde{q}}^T\right]^T = 0 \in \mathbb{R}^{2n}$ of the closed-loop equation is globally uniformly asymptotically stable and therefore :

$$\lim_{t\to\infty} \dot{\tilde{q}}(t) = 0\,, \quad \lim_{t\to\infty} \tilde{q}(t) = 0$$

For practical purposes, the design matrices $K_p$ and $K_V$ may be chosen to be diagonal. This means that the closed-loop equation (3.9) represents a decoupled multivariable linear system that is, the dynamic behavior of the errors of each joint position is governed by second-order linear differential equations which are independent of each other. In this case the selection of the matrices $K_P$ and $K_V$ may be made specifically as:

$$K_P = \text{diag}\left\{\omega_1^2, ....., \omega_n^2\right\}, \quad K_V = \text{diag}\left\{2\omega_1, ....., 2\omega_n\right\}$$

With this choice, each joint responds as a critically damped linear system with bandwidth $\omega_i$. The bandwidth $\omega_i$ defines the velocity of the joint in question and consequently, the decay exponential rate of the errors $\tilde{q}(t)$ and $\dot{\tilde{q}}(t)$. Therefore, in view of these we may not only guarantee the control objective but we may also govern the performance of the closed-loop control system.

### 3.5. Partial Feedback Linearization

Linearizing the state equations does not necessarily linearize the output equation. The idea in partial feedback linearization is to obtain a simple and direct relationship between the system output y and input u. If one needs to differentiate the output of a nonlinear system r times to obtain an explicit relationship between u and y, the system is said to have a relative degree r. This is consistent with the notion of relative degree in linear systems (excess of poles over zeros). If the relative degree is less than the degree of state equations, i.e., r < n, then a part of the system dynamics called the "internal dynamics" has been rendered unobservable in the partial feedback linearization; and the system is not input-state linearizable but partial feedback linearizable. When r = n, there is no internal dynamics; and the system is both input-state and partial feedback linearizable. In order for the closed-loop system to be stable, the internal dynamics must be stable. It is possible for one choice of output to yield a stable internal dynamics while another choice would lead an

unstable one. Therefore, if possible, one should choose the output y ("designer output") such that the internal dynamics is stable

Fully actuated robots are feedback linearizable by nonlinear feedback. For underactuted robots it is known that the portion of the dynamics corresponding to the actuated (or active) degrees of freedom may be linearized by nonlinear feedback. It is named as collocated feedback linearization. Collocated linearization refers to a control that linearizes the equations associated with the actuated degrees of freedom $q_1$ if we consider our underactuated manipulator which has only one actuator on the shoulder joint. The remaining portion of the dynamics after such partial feedback linearization is nonlinear and represents internal dynamics. It is alternatively possible to linearize the portion of the dynamics corresponding to unactuated (or passive) degrees of freedom under a condition which we call strong inertial coupling. In this case the linearization is called as non-collocated feedback linearization which refers to linearizing the passive degrees of freedom [22].

### 3.6.Control of the Manipulator Links via Partial Feedback Linearization

The task of this section is to derive the partial feedback control for the underactuated manipulator. To see a general derivation of partial feedback linearization please refer to [23] and [24].

The motion equations of the manipulator are given by Equations (2.15)-(2.17). Performing the matrix and vector multiplications, the motion equations can be written as :

$$m_{11}\ddot{q}_{11} + m_{12}\ddot{q}_2 + h_1(q,\dot{q}) = u \tag{3.17}$$

$$m_{21}\ddot{q}_{11} + m_{22}\ddot{q}_2 + h_2(q,\dot{q}) = 0 \tag{3.18}$$

Because the manipulator is a planar two-link robot with an actuator at the shoulder (joint 1) but no actuator at elbow (joint 2), the Link 2 is underactuated. That is, only one torque u is applied at the shoulder of the manipulator. Refer to the dynamics of the manipulator derived in the following section, one can see that with setting the input torque u as some desired value determined by the feedback control law, either one link of the manipulator could be controlled to move a given position but not

both. This is the reason why this method is called the partial feedback linearization method. If the system is fully actuated, there are actuators not only at the shoulder but also at the elbow, one can fully linearize the dynamics of both degrees of freedom by feedback control law. As a result, both links could be fully controlled to track given trajectories. this is the so called fully linearization method or the computed torque method.

### 3.6.1. Control of the First Link

At first, one can choose to linearize the collocated degree of freedom $q_1$. The dynamical equation for the manipulator can be written as follows:

$$\ddot{q} = M^{-1}(q)\{-h(q,\dot{q}) + \tau\} \tag{3.19}$$

Expanding the above equation, it is also rewritten by

$$\ddot{q}_1 = \frac{m_{22}}{D} h_1 + \frac{m_{12}}{D} h_2 + \frac{m_{22}}{D} \tau_1 \tag{3.20}$$

$$\ddot{q}_2 = \frac{m_{12}}{D} h_1 - \frac{m_{11}}{D} h_2 - \frac{m_{22}}{D} \tau_1 \tag{3.21}$$

where D is the determinant of the inertia matrix M(q) given by :

$$D = m_{11}m_{22} - m_{12}^2 \tag{3.22}$$

Now one can give the system input u for equation (3.20) as follows :

$$u = \frac{D}{m_{22}}(v_1 + \frac{m_{22}}{D} h_1 - \frac{m_{12}}{D} h_2) \tag{3.23}$$

where $v_1$ is the auxiliary input to the system.

This results in the following system

$$\ddot{q}_1 = v_1 \tag{3.24}$$

$$m_{22}\ddot{q}_2 + h_2(q,\dot{q}) = -m_{21}v_1 \tag{3.25}$$

Since equation (3.24) is now linear, a computed torque controller with feedforward acceleration could be applied for the purpose of the Link 1's position control :

$$v_1 = \ddot{q}_{d1} + K_{v1}(\dot{q}_{d1} - \dot{q}_1) + K_{p1}(q_{d1} - q_1) \tag{3.26}$$

where $q_{d1}$ is the desired value of $q_1$.

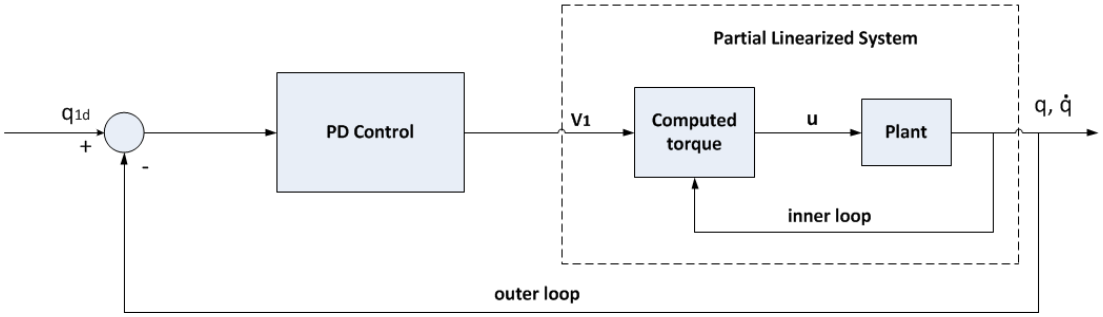


**Figure 3. 1.** Block diagram of the partial feedback linearization control

This is the outer loop control which is employed to move to a desired angle value $q_1$ for Link 1. The response of Link 2 is then given by the resulting nonlinear equation (3.25). Equation (3.25) represents internal dynamics with respect to an output $y = q_1$ . the function of the outer loop control therefore is to move a given angle value for Link 1 and the same time excite the internal dynamics to any angle value for Link 2. First, the state variables, $q_1$, $q_2$, $\dot{q}_1$, $\dot{q}_2$, are fed back to the outer loop control law to calculate the variable $v_1$ (using the equation (3.26)). Then, $v_1$ is used with the state variables to calculate the control input for the manipulator based on the inner loop control law (using equation (3.23)). Now one can see that the so called outer loop and inner loop are actually two steps for calculating the control signal u. They are divided in order to be expressed more clearly.

Now, substituting (3.26) into equation (3.24), one can get the error equation:

$$\mathbf{e} = \begin{bmatrix} e_1 \\ e_2 \end{bmatrix} = \begin{bmatrix} q_{d1} - q_1 \\ \dot{q}_{d1} - \dot{q}_1 \end{bmatrix} \tag{3.27}$$

$$\dot{\mathbf{e}} = \begin{bmatrix} \dot{e}_1 \\ \dot{e}_2 \end{bmatrix} = \begin{bmatrix} 0 & 1 \\ -K_{p1} & -K_{v1} \end{bmatrix} \begin{bmatrix} e_1 \\ e_2 \end{bmatrix} \tag{3.28}$$

The values of $K_{p1}$ and $K_{d1}$ must be positive to guarantee the convergence of the error e to zero. With properly chosen $K_p$ and $K_v$, the convergence rate of the errors could be adjusted.

### 3.6.2. Control of the Second Link

In some cases of controlling the underactuated manipulator one can choose to linearize the non-collocated degree of freedom $q_2$. Similar to the analysis for the control of $q_1$, one can get following results for controlling $q_2$ as given in equation (3.21) :

$$\ddot{q}_2 = \frac{m_{12}}{D} h_1 - \frac{m_{11}}{D} h_2 - \frac{m_{22}}{D} \tau_1$$

Now, the system input u (input torque $\tau_1$) could be given as follows :

$$u = -\frac{D}{m_{12}} (v_2 - \frac{m_{12}}{D} h_1 + \frac{m_{11}}{D} h_2) \tag{3.29}$$

where $v_2$ is auxiliary input to the system.

This results in the system

$$\ddot{q}_2 = v_2 \tag{3.30}$$

$$m_{21}\ddot{q}_1 + h_2(q, \dot{q}) = -m_{22} v_2$$

(3.31)

For the purpose of Link 2's stabilization, computed torque controller is applied in the same manner with Link 1,

$$v_2 = \ddot{q}_{d2} + K_{v2}(\dot{q}_{d2} - \dot{q}_1) + K_{p2}(q_{d2} - q_2) \tag{3.32}$$

where $q_{d2}$ is the desired position value or trajectory of $q_2$.

Now , together with the equation (3.30), one can get the error equation :

$$\mathbf{e} = \begin{bmatrix} e_1 \\ e_2 \end{bmatrix} = \begin{bmatrix} q_{d2} - q_2 \\ \dot{q}_{d2} - \dot{q}_2 \end{bmatrix} \tag{3.33}$$

$$\dot{\mathbf{e}} = \begin{bmatrix} \dot{e}_1 \\ \dot{e}_2 \end{bmatrix} = \begin{bmatrix} 0 & 1 \\ -K_{p2} & -K_{v2} \end{bmatrix} \begin{bmatrix} e_1 \\ e_2 \end{bmatrix} \tag{3.34}$$

With properly chosen $K_{p2}$ and $K_{v2}$, one can adjust the convergence rate of the errors to zero.

Now, it has been proved that any degree of freedom of the underactuated manipulator can be fully controlled very well.

### 3.7. Combining and Implementing the Controllers

In order to control each link of the underactuted manipulator, partly stable controllers are designed. In this case a supervisory controller is needed to control the position of end point of second link. Therefore, a logic based switching controller is proposed which uses position and velocity errors of the joints.

Let us consider n-degrees-of-freedom system in which m joints are active (actuated) where m < n in our case. If a computed torque method is used as a partly stable controller, then the number of states stabilized by the controller is just 2m. When we use a two-link underactuated manipulator with a single actuator, n = 2 and m = 1. Therefore we need two partly stable controllers are needed [25].

#### 3.7.1. Design of Partly Stable Controllers

In the previous sections collocated and non-collocated partial feedback linearized system was controlled with computed torque control method. We can use computed torque control method can be used as a partly stable controller. To do that, first the equations for stabilization of the first link are recalled. Joint 1 acceleration equation is obtained from the dynamic model in the previous parts as follows :

$$\ddot{q}_1 = \frac{m_{22}}{D} h_1 + \frac{m_{12}}{D} h_2 + \frac{m_{22}}{D} \tau_1$$

Then for the computed torque controller for stabilizing only $q_1$, letting the desired angle be $q_{d1}$, its angular velocity be $\dot{q}_{d1}$, the propotional gain be $K_{p1}$, derivative gain be $K_{v1}$, and the modified angular acceleration be given by :

$$v_1 = \ddot{q}_{d1} + K_{v1}(\dot{q}_{d1} - \dot{q}_1) + K_{p1}(q_{d1} - q_1)$$

It follows that

$$\tau_1 = \frac{D}{m_{22}}(v_1 + \frac{m_{22}}{D}h_1 - \frac{m_{12}}{D}h_2)$$

Similarly, the computed torque controller for stabilizing only $q_2$ is reduced to following equations as given in non-collocated partial feedback linearization section:

$$v_2 = \ddot{q}_{d2} + K_{v2}(\dot{q}_{d2} - \dot{q}_1) + K_{p2}(q_{d2} - q_2)$$

$$\tau_1 = -\frac{D}{m_{12}}(v_2 - \frac{m_{12}}{D}h_1 + \frac{m_{11}}{D}h_2)$$

### 3.7.2. Switching Control

Since the system has only one actuator at the shoulder joint a supervisory switching controller is needed to decide which controller must be chosen in order to reach desired end point position. For that purpose a logic based switching algorithm is defined by using joint error energies. Energy is defined by using generalized coordinates. Desired joint angle of each link is $q_{di}$, and the error of joint angle is denoted by :

$$e_i \triangleq q_{di} - q_i \tag{3.35}$$

Then, the energy of each link is defined by

$$E_i \triangleq e_i^2 + \dot{e}_i^2 \tag{3.36}$$

Let the partly stable controller that stabilizes only the i-th link be denoted by $C_i$. If the controller $C_1$ is adopted, then $E_1$ is decreased while $E_2$ is increased, because $q_1$ can be stabilized by its controller. Similarly, if the controller $C_2$ is adopted, then $E_2$ is decreased while $E_1$ is increased.

Considering the energy functions for the joints, in order to achieve predefined state values which are angles and velocities of both joints and to make defined energies zero which means reaching to the desired points with zero velocity, a logic based switching function can be defined as follows:

$$\hat{\mathrm{I}} = \begin{cases} 1 & \text{if } \mathrm{E}_1 > \mathrm{E}_2 \\ 2 & \text{if } \mathrm{E}_1 \le \mathrm{E}_2 \end{cases} \tag{3.37}$$

where $\hat{\mathrm{I}}$ is the switching index number that decides which controller needs to be chosen according to error energies of joints. Figure 3.2. shows the block diagram structure of controlled system.

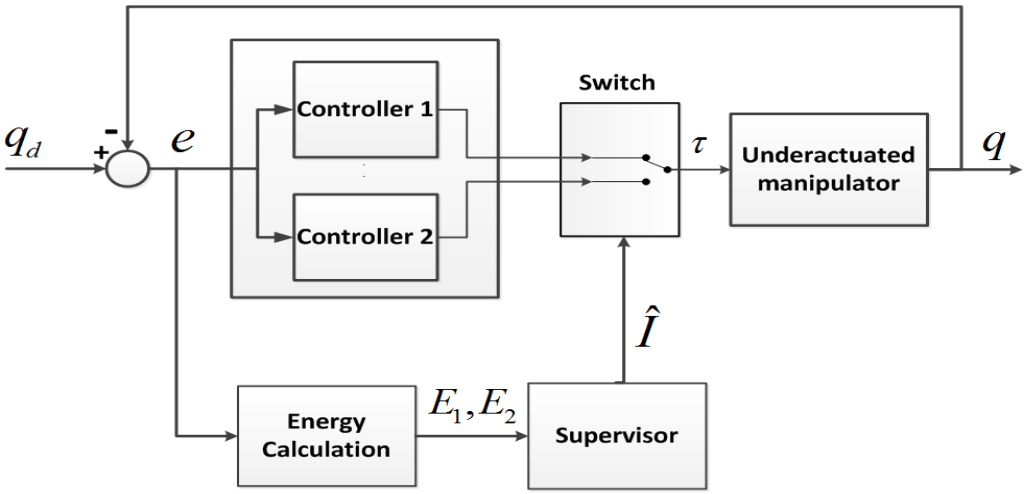


**Figure 3. 2.** Block diagram of the proposed switching control system

# CHAPTER IV

# SIMULATION RESULTS

After theoretical analysis of the underactuated manipulator and designing a control algorithm for the system it is necessary to observe controller performance. To do that, firstly, a simulation in the computer is needed. The powerful built-in toolbox in Matlab, called Simulink, is used to simulate two-link underactuated manipulator system. Simulink is a software package for modelling, simulating and analyzing dynamical systems. It supports linear and nonlinear systems, modelled in continous time, sampled time, or a hybrid of the two [26].

## 4.1. Simulation of Underactuated Manipulator

The physical description of the system we study on was given in Figure 2.1. There are two ways of simulating this system in Simulink environment. First we can model the system by using its dynamical equations given in the state space form in equation (2.21). Figure 4.1 illustrates the model of underactuated manipulator.

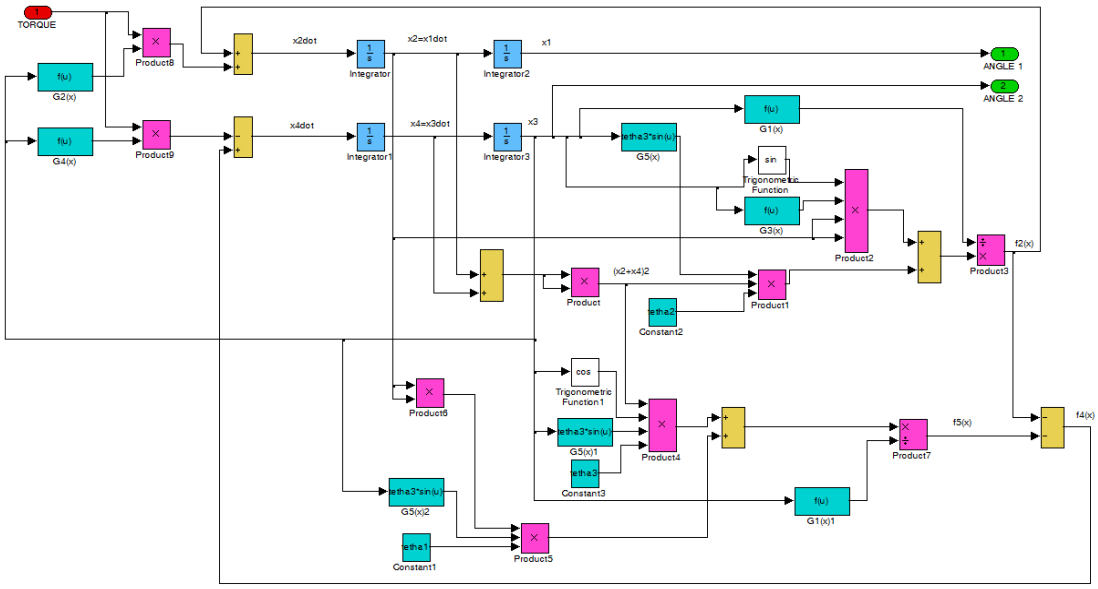


**Figure 4. 1.** Mathematical model based system model in Simulink

In the second way, the system is simulated using Simmechanics toolbox which has simple compact mechanical component blocks. By using these blocks one can realize the whole system simply and achieve the same system dynamical behaviour. For the sake of simplicity of the system, in control design steps and observation of the system performance Simmechanics based model is used. Figure 4.2 shows the same system which is made up in Simmechanics toolbox.

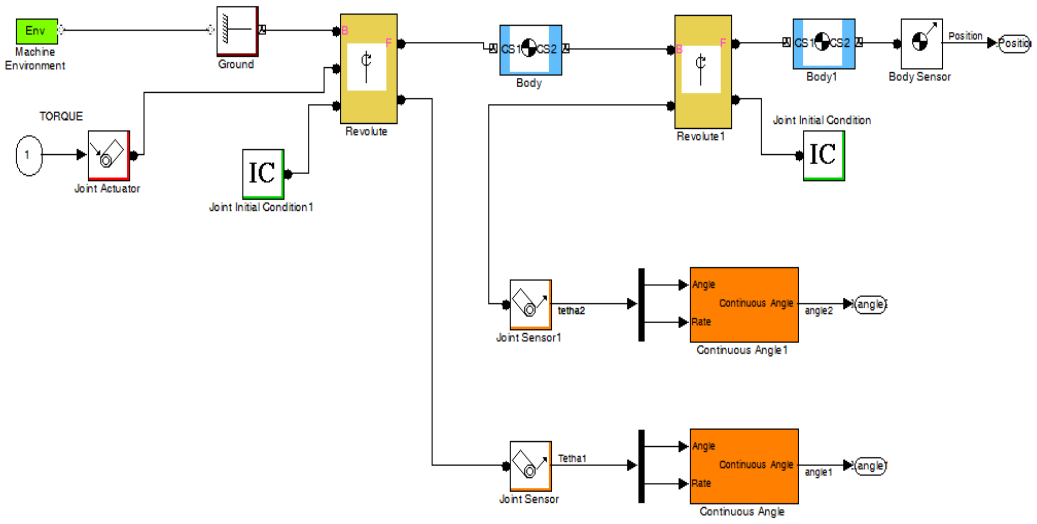


**Figure 4. 2.** Mechanical representation of the system in Simmechanics toolbox

For validation of the model given in Figure 4.2, both systems are compared for the same input torque which is given in Figure 4.3. Simulation sample time is chosen as 0.001 s and total simulation time is 1 s. Total simulation time is kept small since second link in this case has high frequency oscillations and not clearly seen. Input torque is given in a 0.2 s duration. The output response of dynamical model based simulation and Simmechanics based systems are exactly the same as shown in Figure 4.4.

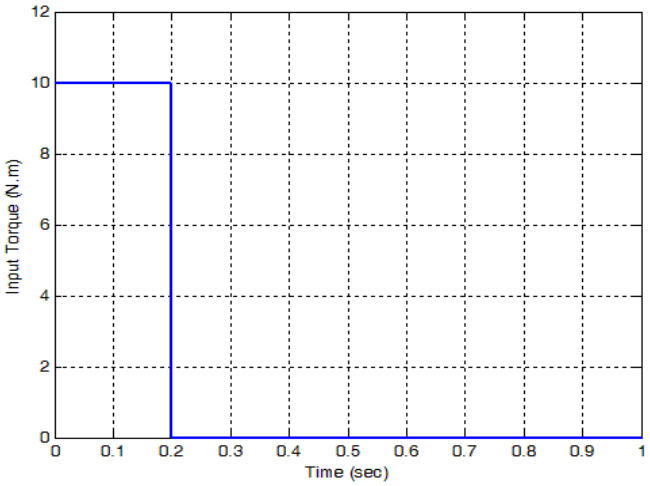


**Figure 4. 3.** Applied torque to the compared systems

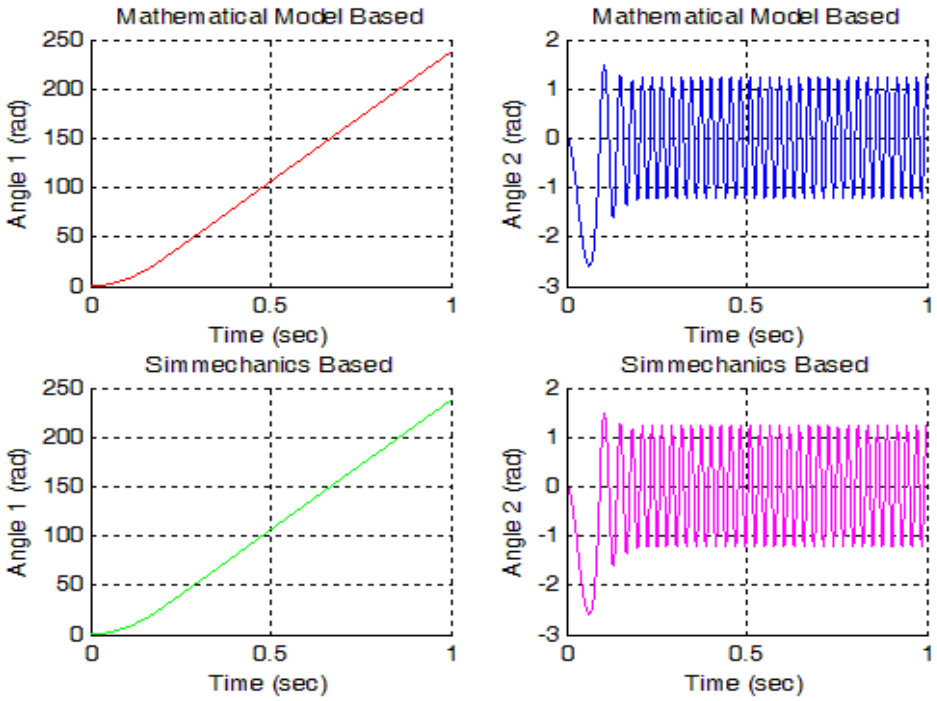


**Figure 4. 4.** Mathematical model and Simmechanics based system outputs

### 4.2. Simulation of the Combined System

In practice, joint friction cannot be neglected in underactuated robotic manipulators, especially at the passive joint. This is because while friction at the active joints can be directly compensated, the same is not true for the passive joint [27]. Since we implement the control algorithm to a real system, in the simulation of the manipulator, joint friction of free joint is considered. Therefore static and viscous friction of the second joint is included in H(q, $\dot{q}$) matrix which is given in equation

(2.17) and controller is designed considering frictions. Frictions are also considered in mechanical realization of the system in Simmechanics and model is modified according to the joint frictions. Modified model of the system can be seen in Figure 4

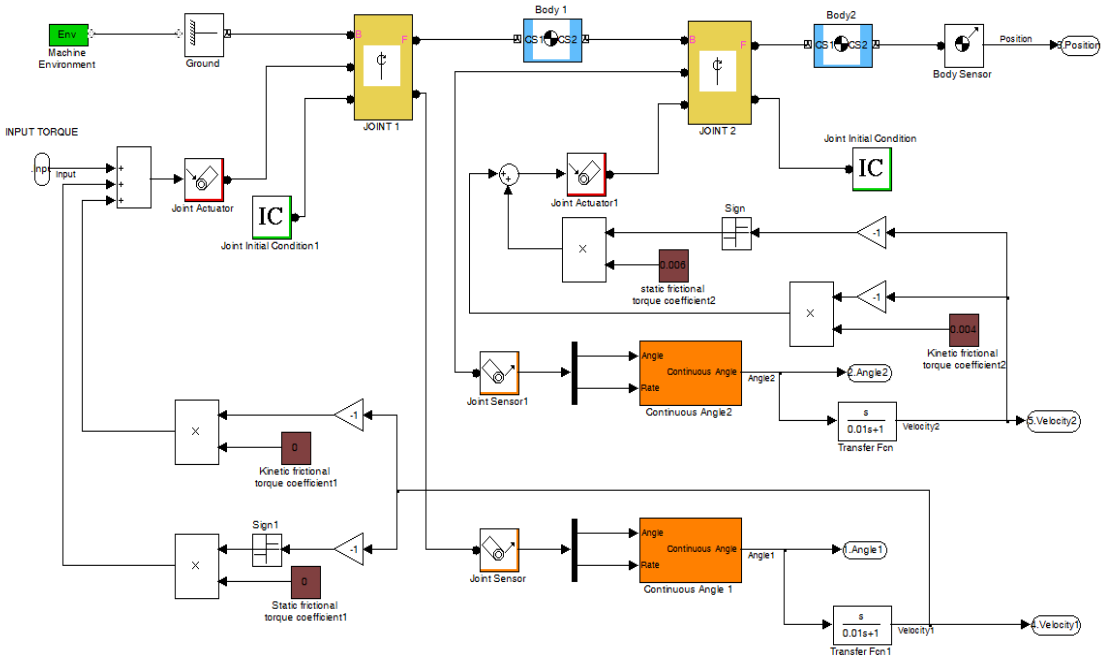


**Figure 4. 5.** Manipulator system with joint frictions

For the stabilization of first joint, computed torque controller with partial feedback linearization is adobted to the simulated system by using Equations (3.24) - (3.26) . Figure 4.6 shows block structure of Controller 1.

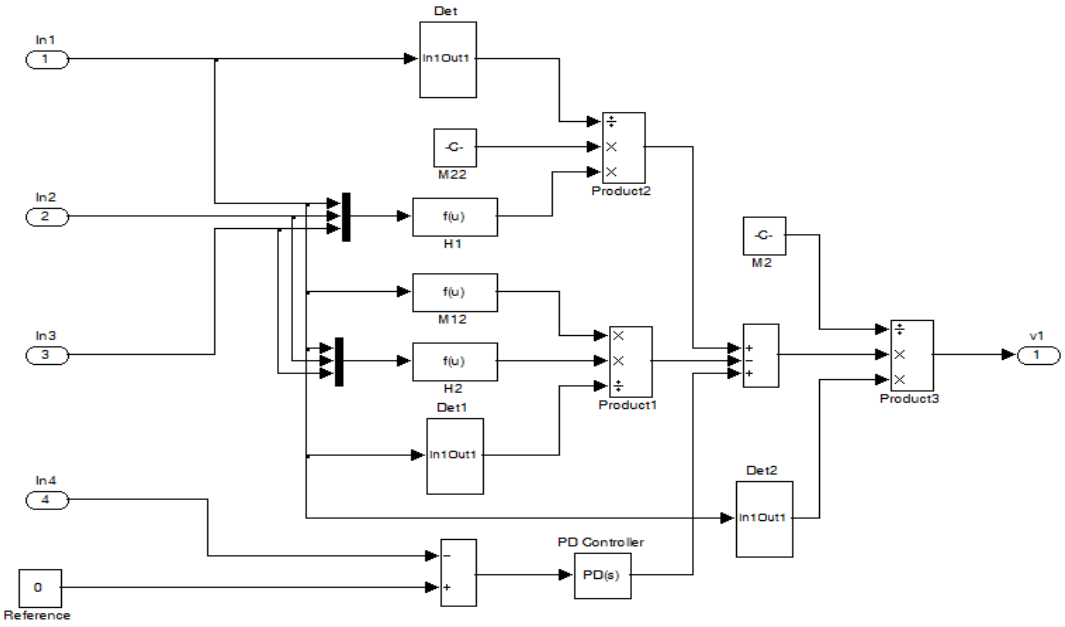


**Figure 4. 6.** Simulink model of the controller which stabilizes the first joint

In the same manner, the controller that stabilizes only second link is made up based on Equations (3.30) - (3.32) as shown in Figure 4.7

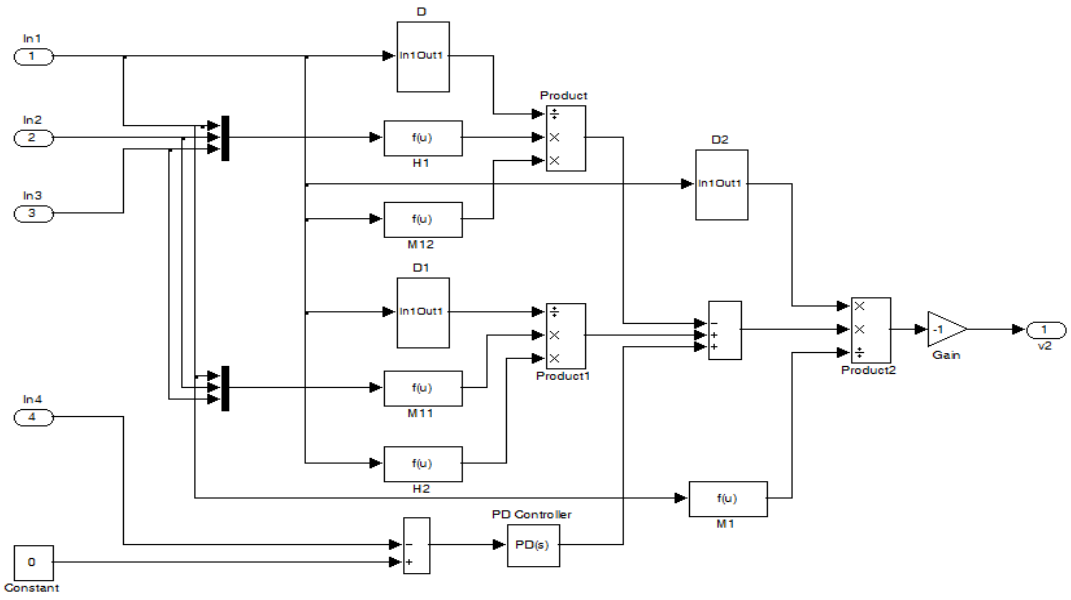


**Figure 4. 7.** Simulink model of the controller which stabilizes the second joint

In order to calculate the error energies of joints, an energy calculation subsystem is designed and integrated to the controller. Then, this subsystem is adopted to supervisor, and with the controllers, constitutes switching controller. Figure 4.8 illustrates the combined system simulation.

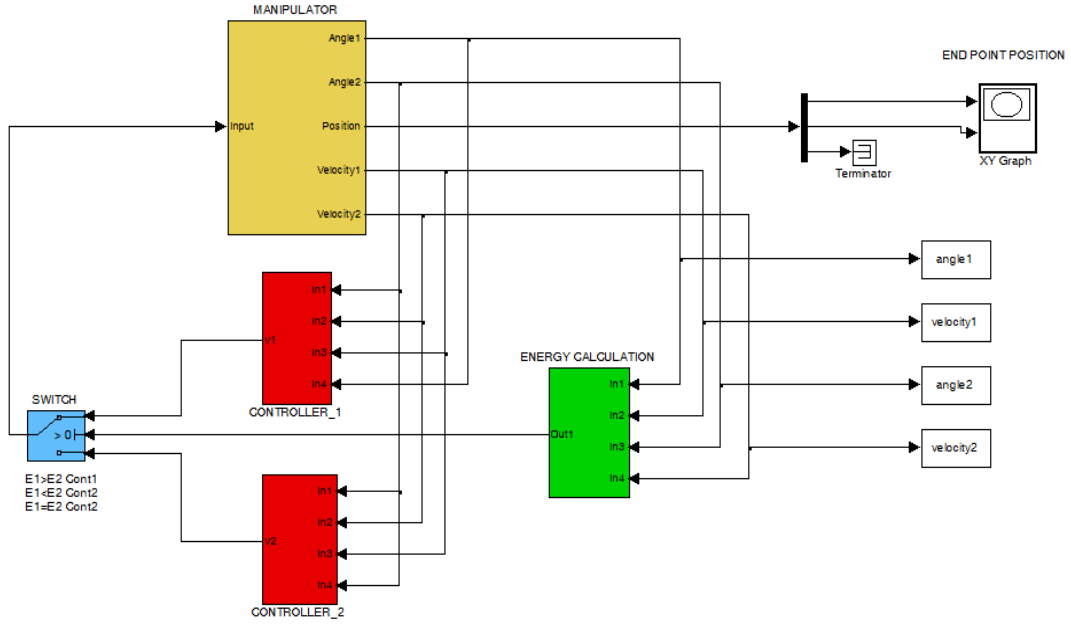


**Figure 4. 8.** Controlled manipulator system simulation in Simulink

**Table 4. 1.** Manipulator parameters used in the simulation

| Parameter | Parameter Values |
|---|---|
| $m_1$, $m_2$ | 0.12[kg], 0.05[kg] |
| $l_1$, $l_2$, $r_1$, $r_2$ | 0.1[m],0.15[m],0.0976[m],0.09[m] |
| $I_1$, $I_2$ | 0.005[kgm$^2$], 0.0002[kgm$^2$] |
| $f_{v1}$, $f_{v2}$ | 0[Nms], 0.006[Nms] |
| $f_{s1}$, $f_{s2}$ | 0[Nms], 0.004[Nms] |

Since we apply the designed control system to a prototype of underactuted manipulator, in the simulation part, physical parameters of this real system is used as given in Table 4.1. It may be useful to select the desired responses at the end of the arm faster than the base, where the masses that must be moved are heavier. It is undesirable for the partly stable controllers to exhibit overshoot since this colud cause impact if fast swicthing between controllers occurs and settling time in the position control increases. Therefore the PD gains are usually selected for critically damping $\zeta = 1$. The natural frequency $\omega_n$ governs the speed of rensponse in each error component. It should be large for fast responses and is selected depending on the performance objctives. Another upper bound on $\omega_n$ is provided by considerations on actuator satuaration. If the PD gains are too large the input torque mat reach its upper limit. Considering the conditions mentioned above and joint velocity range of joints in real system, gain parameters of partly stable controllers are adjusted to the suitable values. Each gain parameters were fixed during several explorations to $K_{p1} = 49.0$, $K_{v1} = 14$, $K_{p2} = 225.0$, $K_{v2} = 30.0$ where $K_{pi}$ is the proportional gain of *i*th link and $K_{vi}$ is the derivative gain.

Firstly, for the purpose of observing individual controller performance, only one of the partly stable controllers is applied to the systems. The state vectors are defined as joint angles and velocities in the following form :

x : $x_1 = q_1$, $x_2 = \dot{q}_1$, $x_3 = q_2$, $x_4 = \dot{q}_2$

Then if only controller 1 is adopted to the system which means control objective is to bring the first joint to a given $q_{d1}$ with zero velocity and final position of the second joint is not specified. With this controller only first link of manipluator can be controlled as mentioned in previous chapters. In this case one can choose desired state vector as $x_d = \begin{bmatrix} 0 & 0 & q_{2f} & 0 \end{bmatrix}^T$, where $q_{2f}$ is the final position of second joint which is not specified. In order to see controller performance two inital state vectors are chosen as follows:

$$x_i(0) = \begin{bmatrix} q_1(0) & \dot{q}_1(0) & q_2(0) & \dot{q}_2(0) \end{bmatrix}^T$$

$$x_1(0) = \begin{bmatrix} 2 & 0 & 0 & 0 \end{bmatrix}^T$$

$$x_2(0) = \begin{bmatrix} 3 & 0 & -1 & 0 \end{bmatrix}^T$$

For the specified initial conditions variation of angles of underactuated manipulator with time can be seen in Figure 4.9 and 4.10. Sampling interval of the simulations is chosen as 0.01 s and total simulation time is 5 s.

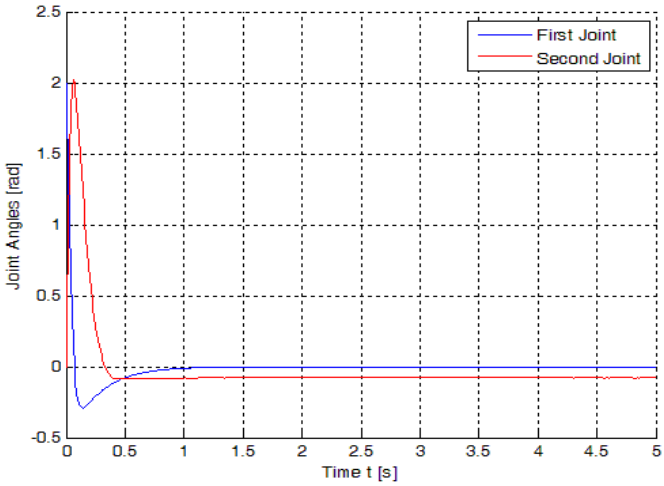


**Figure 4. 9.** Controller 1 adopted system angle changes for $x_1(0)$ inital state vector

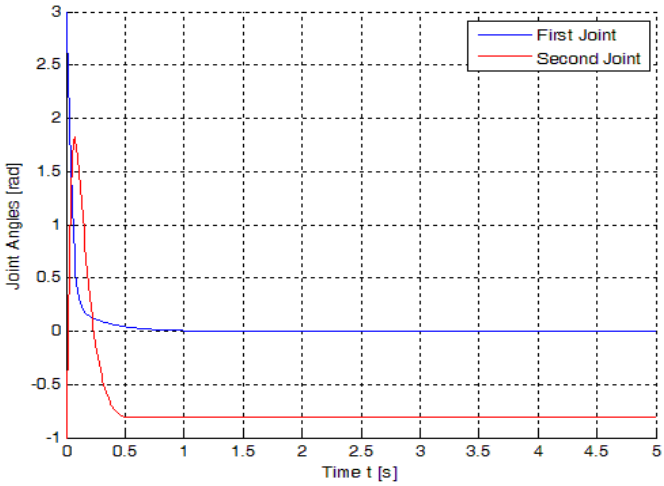


**Figure 4. 10.** Controller 1 adopted system angle changes for $x_2(0)$ inital state vector

From Figure 4.9 and 4.10, it can be seen that Controller 1 stabilizes the first joint position while second joint reaches and stay at any position value.

In the same manner, only Controller 2 can be adopted to the system with the desired state vector $x_d = [q_{1f} \quad 0 \quad 0 \quad 0]^T$ where $q_1$ position is not specified. For the purpose of examining the controller system, two inital conditions are given as follows:

$$x_1(0) = [-1 \quad 0 \quad 1 \quad 0]^T$$

$$x_2(0) = [-1 \quad 0 \quad 2 \quad 0]^T$$

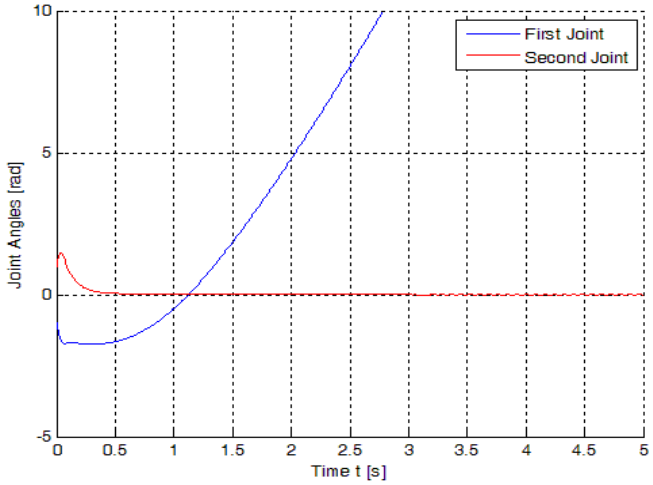


**Figure 4. 11.** Controller 2 adopted system angle changes for $x_1(0)$ inital state vector

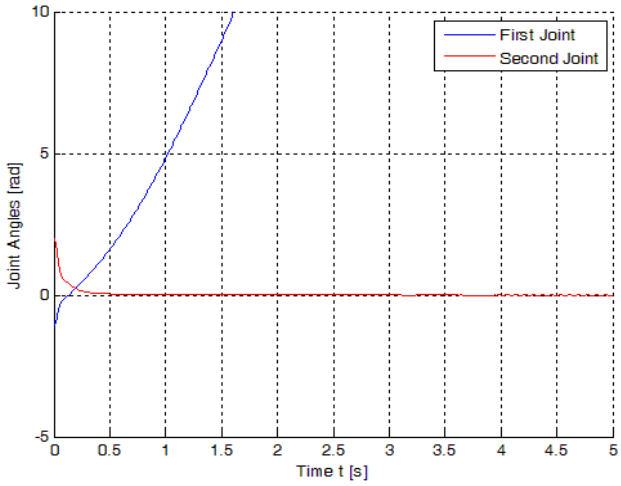


**Figure 4. 12.** Controller 2 adopted system angle changes for $x_2(0)$ inital state vector

As we can see from Figure 4.11 and Figure 4.12, if only Controller 2 is used, second joint position can be controlled while first joint reaches any random position value.

Finally, we examine fully controlled system performance. We combine two controllers with switching rule and stabilize both joints. The objective of state feedback controller is to bring angles of two joints to predefined positions with zero velocity. To this end, simulation sampling interval is adjusted to 0.01 s and total simulation time is adjusted to 30 s and desired state vector is defined as $x_d = \begin{bmatrix} 0 & 0 & 0 & 0 \end{bmatrix}^T$. Initial state vectors used in the simulations are as given below :

$$x_1(0) = \begin{bmatrix} 2 & 0 & 0 & 0 \end{bmatrix}^T$$

$$x_2(0) = \begin{bmatrix} 0 & 0 & 2 & 0 \end{bmatrix}^T$$

$$x_3(0) = \begin{bmatrix} 2 & 0 & 2 & 0 \end{bmatrix}^T$$

### 4.3. Results and Discussion

For initial condition $x_1(0) = \begin{bmatrix} 2 & 0 & 0 & 0 \end{bmatrix}^T$, Figure 4.13 - 4.15 shows variations of manipulator joint angles, velocities and input torque with time. It can be seen that both joints reach desired position values quickly with a very small error. Also for initial conditions $x_2(0) = \begin{bmatrix} 0 & 0 & 2 & 0 \end{bmatrix}^T$ and $x_3(0) = \begin{bmatrix} 2 & 0 & 2 & 0 \end{bmatrix}^T$,Figure 4.16-

4.18 and Figure 4.19-4.21 shows these variation for each initial condition respectively. The settling time of joint positions and torque needed to stabilize the joint positions changes according to initial configuration and desired state vector. If initial errors of the joints increases, settling time and total applied torque also increase. It is clearly seen if we look at the system responses for initial state vector $x_3(0)$. It is also shown that the errors are kept within a small varying range, and converge to zero quickly. Because of the switching control the error values always oscillate in a very small range around zero.

Using PD controller at the outer loop control of partly stable controllers is very effective if all the manipulator parameters are known and there is no disturbance. In the presence of constant disturbances, PD control gives a nonzero steady-state error. A common modification is to add an integrator term to eliminate steady-state errors. This introduces additional complications since care must be taken to maintain stability and avoid integrator windup. Additionally using a PID controller in partly stable controllers can ruin critically damped response [28]. Since we use continuous and in some cases fast switching between controllers it can increase the settling time and has a negative impact on small amplitude oscillations in the steady state part of position response. Table 4.2 gives the results of output responses in which case one of PD and PID controllers is chosen as the outer loop controller for designing partly stable controllers. Figures 4.22-4.24 shows the joint position responses for three initial conditions given above.

**Table 4. 2.** Comparison of outer loop controller responses

| | **PD Control** | | | **PID Control** | | |
|---|---|---|---|---|---|---|
| | **$X_1(0)$** | **$X_2(0)$** | **$X_3(0)$** | **$X_1(0)$** | **$X_2(0)$** | **$X_3(0)$** |
| Maximum Overshoot (%) | 100 | 100 | 350 | 125 | 110 | 350 |
| Settling Time (second) | 4 | 5 | 5 | 10 | 17 | 18 |
| Steady-state Error (radian) | 0.01 | 0.01 | 0.015 | 0.02 | 0.015 | 0.01 |

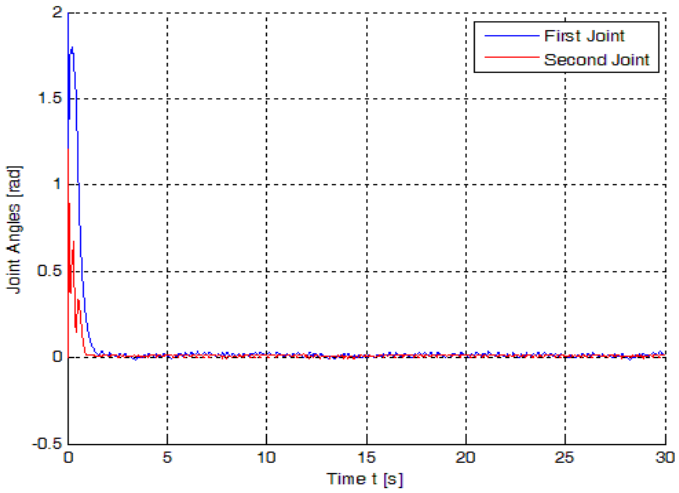


**Figure 4. 13.** Joint angle outputs of controlled system for initial condition $x_1(0)$

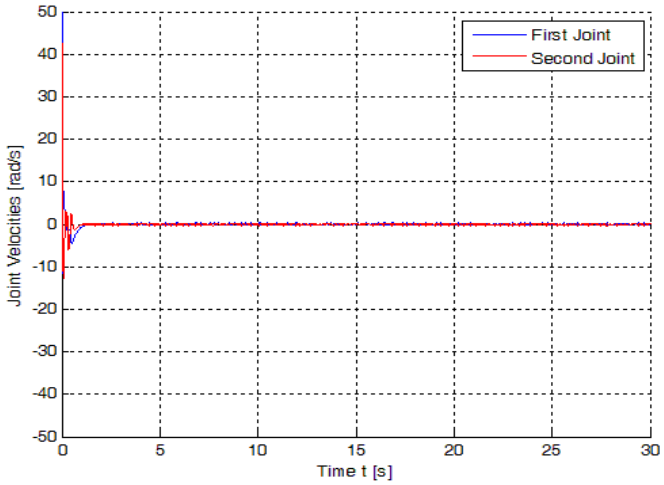


**Figure 4. 14.** Joint velocity outputs of controlled system for initial condition $x_1(0)$

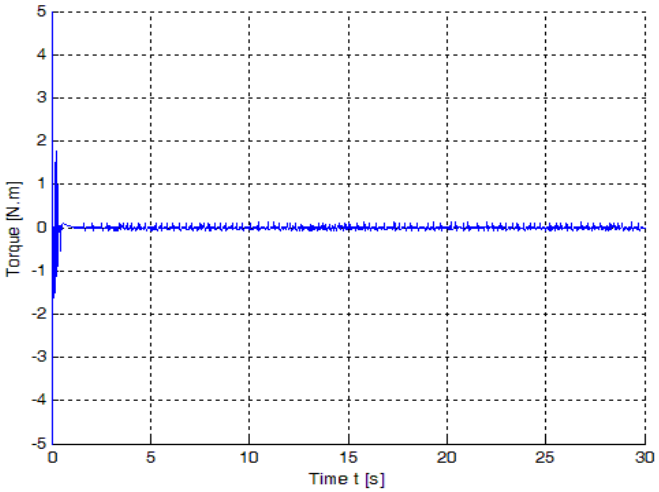


**Figure 4. 15.** Input torque applied to the first joint initial condition $x_1(0)$

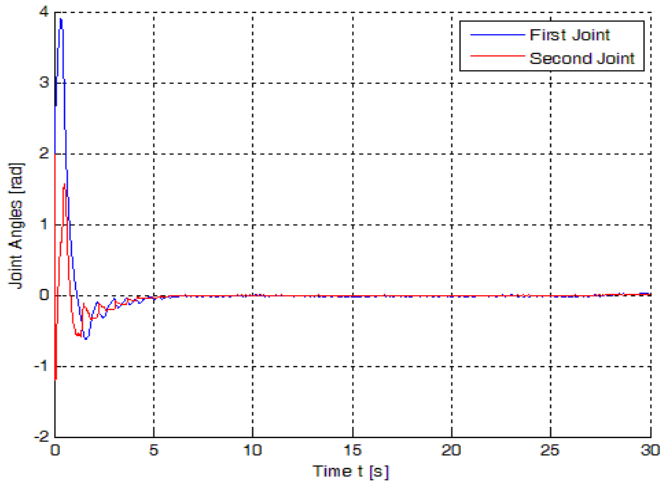


**Figure 4. 16.** Joint angle outputs of controlled system for initial condition $x_2(0)$

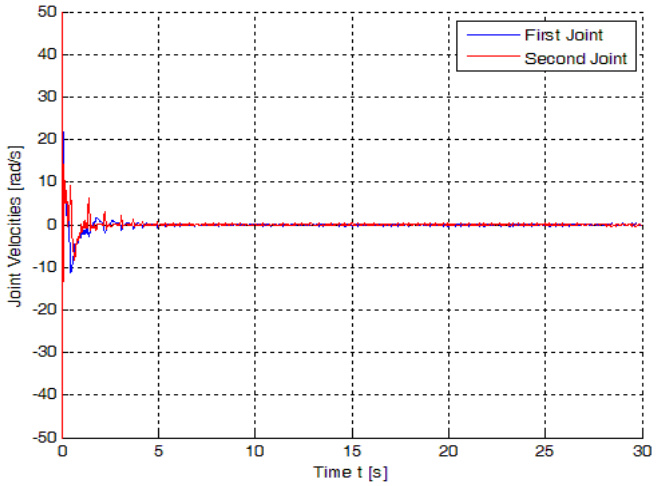


**Figure 4. 17.** Joint velocity outputs of controlled system for initial condition $x_2(0)$

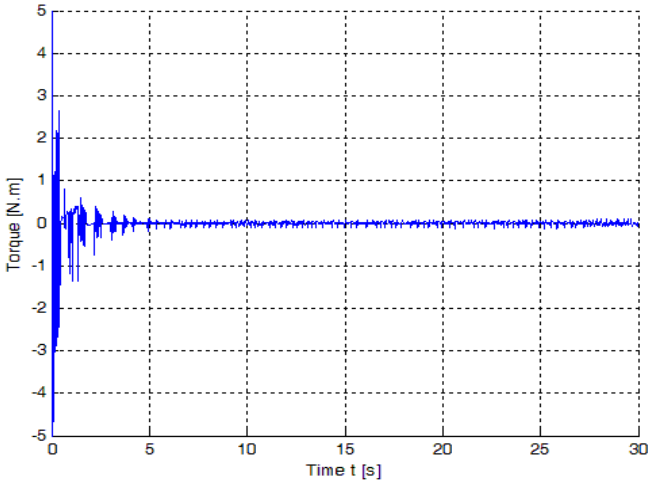


**Figure 4. 18.** Input torque applied to the first joint initial condition $x_2(0)$

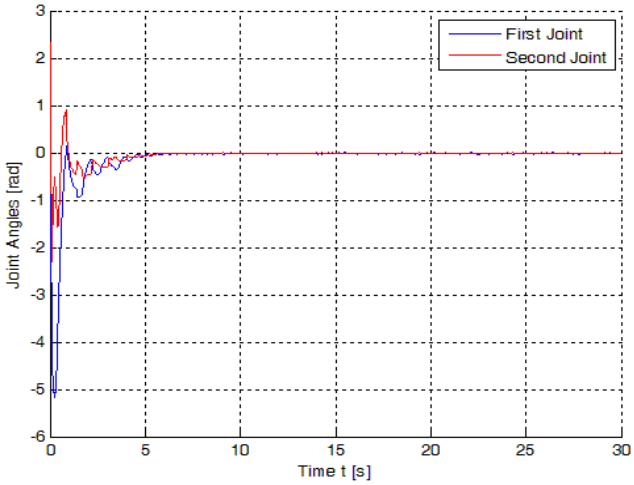


**Figure 4. 19.** Joint angle outputs of controlled system for initial condition $x_3(0)$

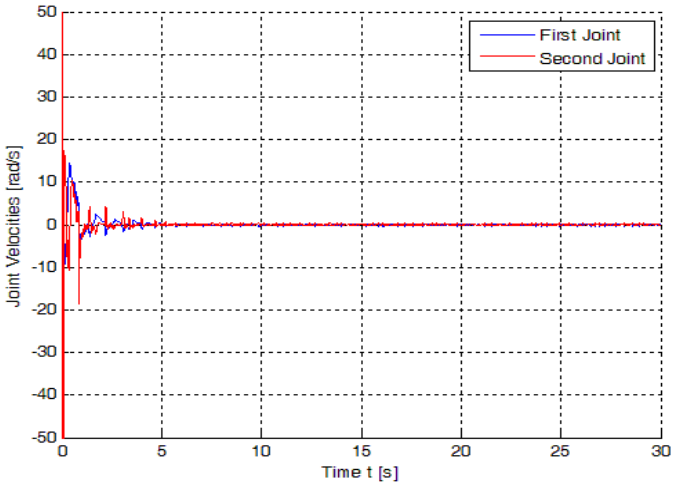


**Figure 4. 20.** Joint velocity outputs of controlled system for initial condition $x_3(0)$

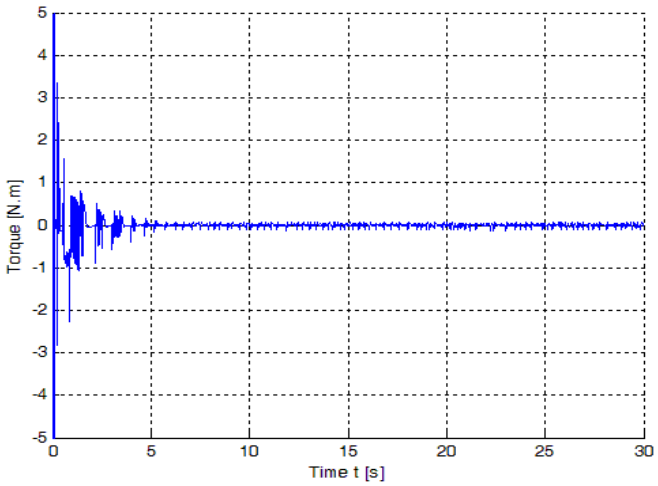


**Figure 4. 21.** Input torque applied to the first joint initial condition $x_3(0)$

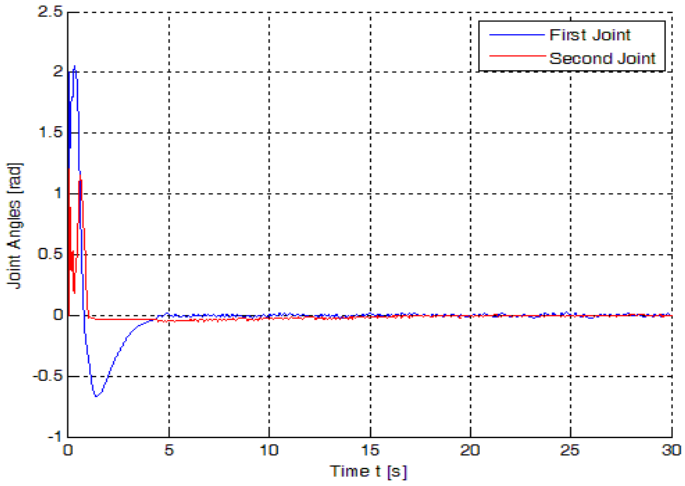


**Figure 4. 22.** Joint angle outputs of PID controlled system for intial $x_1(0)$

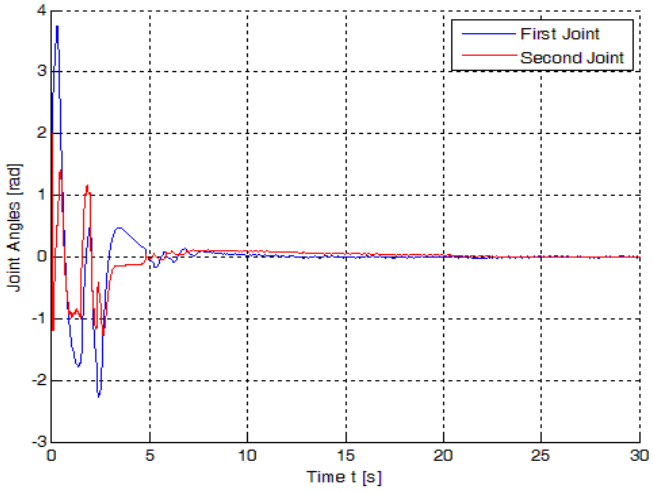


**Figure 4. 23.** Joint angle outputs of PID controlled system for intial $x_2(0)$

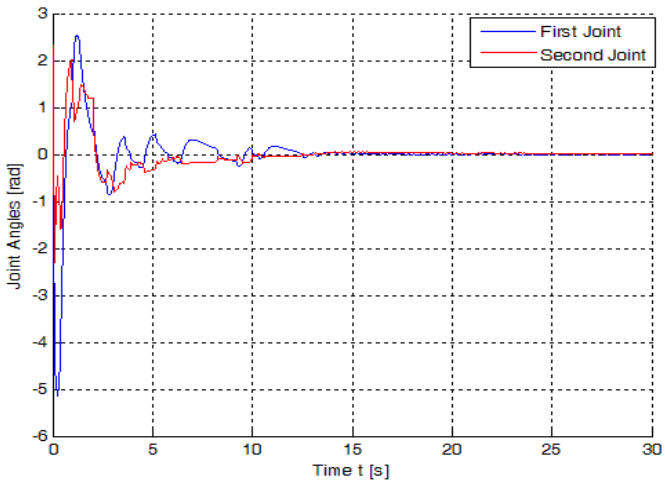


**Figure 4. 24.** Joint angle outputs of PID controlled system for intial $x_2(0)$

# CHAPTER V

# EXPERIMENTAL SETUP AND RESULTS

## 5.1. Introduction

This chapter investigates the real-time implementation of the underactuated horizontal manipulator with state feedback controller applied to it. The term “real-time” has been applied to many types of systems including computer-controlled power stations, flight-control software, and robot control. Real-time is the operation of a computer system in which the programs for the processing results are available within a given time interval. Depending on the application, the data may appear at unknown or predetermined time [29].

Due to the advent of inexpensive and fast computers, the implementation of the algorithms on hardware is becoming convenient and practical. However, most research was based on simulations, and the literature lacks real-time results. Theoretical analysis and computer simulation of the combined system are important but not sufficient in that inherent factors such as unmodeled high frequency dynamics and measurement noise are usually neglected for stability analysis in the simulation [25]. Therefore, the ultimate justification for the value and applicability of controllers should be proved in the actual hardware implementation of the combined system. Based on this perspective, this chapter examines the real-time performance of the underactuated manipulator system after applying the switching based state feedback controller to it.

## 5.2. Mechanical Design of the Manipulator

A simple two link planar manipulator is constructed to observe real-time performance of the controller. The photography of manipulator is shown in Figure 5.1. Two links are made of aluminum and manipulator has two fully rotational revolute joints. The length of link #1 is selected to be 10 cm; the other dimensions of the link are selected to be 2 cm width and 6 mm thickness. The length of link #2 is

selected to be longer than link #1, to enhance underactuation property of it [22]. Thus it is selected to be 15 cm, the other dimensions of the link are same as link#1.

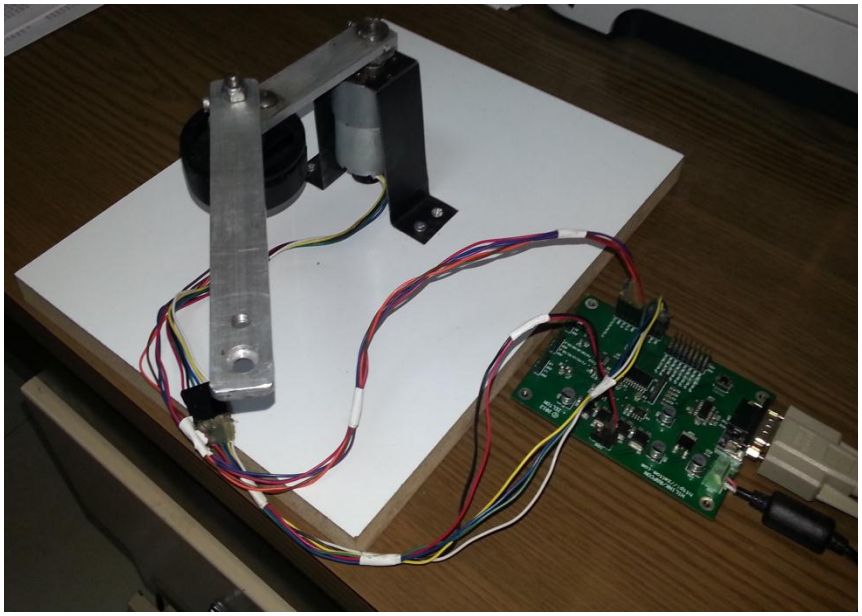

**Figure 5. 1.** Experimental set up for underactuated manipulator

Dc motor is fixed and hanged on motor base and coupled with the first end link#1 (shoulder of the manipulator). The encoder on the passive joint (second joint) is hanged on link#1 and coupled with link#2. That is, the encoder shaft rotates as link#2 rotates and weight of encoder is added to link#1. The geometric and mass properties of manipulator are given in Table 5.1.

**Table 5. 1.** Geometric and mass properties of manipulator

| Parameter | Value | Parameter | Value |
|---|---|---|---|
| $m_1$ | 0.12 kg | $r_1$ | 0.0976 m |
| $m_2$ | 0.05 kg | $r_2$ | 0.0750 m |
| $l_1$ | 0.1 m | $I_1$ | 0.0003167 kg.m$^2$ |
| $l_2$ | 0.15 m | $I_2$ | 0.0002000 kg.m$^2$ |

### 5.3. Combining DC Motor and Manipulator Model

Manipulator has only one actuator at the shoulder joint and is driven by torque input. Therefore, driving torque is provided with a permanent magnet DC motor. Equivalent circuit of the armature-controlled DC motor is given in Figure 5.2. equations of this DC motor are given as [30] :

$$V = R_a i_a + L_a \frac{di_a}{dt} + E_b \tag{5.1}$$

$$\tau_m = k_t i_a = J_m \frac{d\dot{q}_m}{dt} + B_m \dot{q} \tag{5.2}$$

Where $\dot{q}_m$ is the angular speed, $L_a$ is armature inductance, $R_a$ is the armature resistance, $i_a$ is the armature current, $k_t$ is the torque constant, and $E_b$ is the back EMF voltage. According to the energy conservation, the following energy equivalence holds :

$$E_b i_a = \tau_m \dot{q}_m \tag{5.3}$$

It is known that $e_b$ is proportional to the angular speed for some constant $k_e$ as follows :

$$E_b = k_e \dot{q}_m \tag{5.4}$$

From Equations (5.2) and (5.3) it can be obtained that $k_e = k_t$.

Since $L_a$ is small enough to be neglected, equation (5.1) can be simplified and combined with Equation (5.2) [31]. In the end, DC motor torque can be calculated from the following equation:

$$\tau_m = k_t \frac{(V - k_e \dot{q}_m)}{R_a} \tag{5.5}$$

In Figure 5.1, the gear ratio is denoted as n, and the following relationships are known :

$$\frac{q_m}{q_1} = \frac{\dot{q}_m}{\dot{q}_1} = \frac{\tau_1}{\tau_m} = n \tag{5.6}$$

Finally, the relationship between DC motor voltage and input torque needed by the manipulator takes the following form :

$$\tau_1 = k_t \frac{(Vn - k_e \dot{q}_1)}{R_a n^2} \tag{5.7}$$

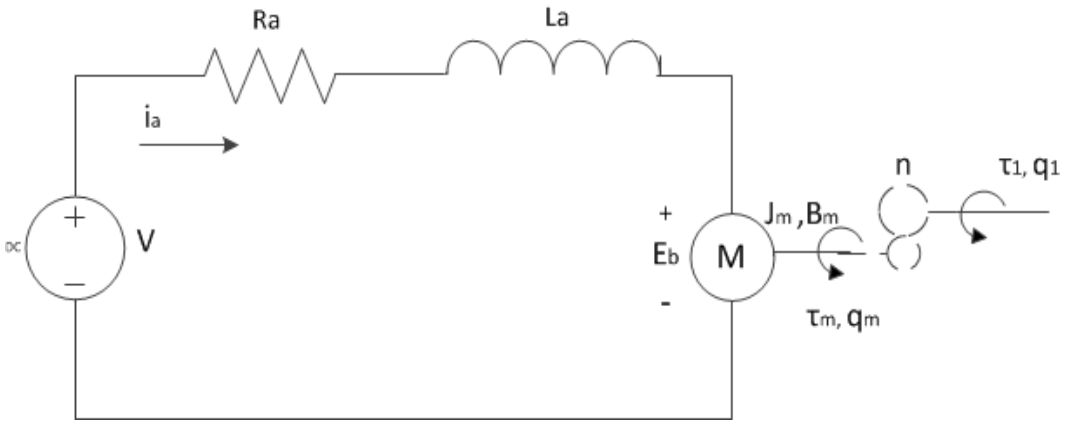


**Figure 5. 2.** Equivalent circuit of permanent magnet DC motor

In prototype manipulator system a 12 V, 5A permanent magnet DC motor is chosen as actuator. It is used with a gearbox so that high torques needed by the manipulator can be supplied. It has 150 rpm free-run speed and 1.41 Nm stall torque at the output of gearbox. DC motor parameters are given in Table 5.2.

**Table 5. 2.** Parameters of permanent magnet DC motor

| | | | |
|---|---|---|---|
| $R_a$ | 2.4 Ω | $k_t$ | $4 \times 10^{-3}$ Nm/A |
| $L_a$ | 0.01 H | $J_m$ | $0.056 \times 10^{-6}$ kgm$^2$ |
| $k_e$ | $4 \times 10^{-3}$ V/rad/s | $B_m$ | $1.6 \times 10^{-6}$ Nm/rad/s |
| n | 1 : 67 | | |

### 5.4. Digital Encoders

To have high precision in the reading of joint angles from digital encoders, resolution of encoders are chosen to be high enough. Both of them are incremental encoders in which initial angle outputs are always zero. Stated otherwise, they can not remember the last position for previous application if we use them again. The encoder used at

the first joint has 16 ppr (pulse per revolution). Since it is coupled with DC motor shaft, at the gearbox output shaft its resolution is multiplied by gear ratio and gives 1072 ppr. For the passive joints which rotates freely, a 1024 ppr optical encoder is used.

### 5.5. Real-Time Control Board

A real-time hardware-in-the-loop control platform for Matlab/Simulink is used to control the manipulator with designed controller on computer. The controller card is capable of giving appropriate control signal to the real system and getting sensor outputs back to the controller on computer.

#### 5.5.1. Specifications

- Power supply: 6 − 15 V, minimum 0.15 A, regulated
- Interface: 115200 baud, 8 bit data, no parity, 1 stop bit
- Analog inputs: A0–A7, 0 − 5 V analog, 12 bit resolution
- Capture inputs: C0–C1, 0 − 5 V digital, 16 bit resolution
- Digital inputs: D0 d0–D0 d7, 0 − 5 V digital, 8 lines
- Encoder inputs: E0–E1, 0 − 5 V digital, 16 bit resolution
- Frequency outputs: F0–F1, 0 − 5 V digital, 16 bit resolution
- Analog outputs: B0–B1, 0 - 5 V analog, 12 bit resolution
- Digital outputs: G0 g0–G0 g7, 0 - 5 V digital, 8 lines
- Pulse outputs: H0–H1, 0 - 5 V digital, 16 bit resolution
- Filtered pulse outputs: L0–L1, 0 - 5 V analog
- H-bridge outputs: P0–P1, 0-(supply voltage) V digital, 5 A
- Voltage regulator output: VDD, 5 V, 0.25 A, regulated power supply
- Ground: GND, 0 V
- Sampling rate: up to 3.8 kHz

The real-time control board is based on a DSPIC30F2012 digital signal controller. It has a total number of 8×16 bit inputs and 8×16 bit outputs capability. The inputs and outputs can be selected among the inputs and outputs listed above. The board is interfaced to the main computer that runs Matlab through a serial port. Two pulse-width modulation driven H-bridges with 5 A drive capability are included on the

board.This feature gives the capability of driving external actuators or loads. The functional block diagram of the board is shown in Figure 1. In the figure, A0–A7 are the analog inputs, B0–B1 are the analog outputs. C0–C1 are the capture inputs, D0 d0–D0 d7 are the digital inputs, E0–E1 are the encoder inputs, F0–F1 are the frequency outputs, G0 g0–G0 g7 are the digital outputs and H0–H1 are the pulse outputs. ADC represents the analog-to-digital converter, DAC represents the digital-to-analog converter. ICM represents the input capture module, OCM represents the output-compare module, DIP represents the digital-input port, DOP represents the digital-output port, QEM represents the quadrature-encoder module and PWM represents the pulse-width modulator. FLs are the lowpass filters with outputs L0–L1 and HBs are the H-bridges with outputs P0–P1. μC is the central microcontroller, UART is the universal-asynchronous-receiver-transmitter unit and PC is the host computer [31].

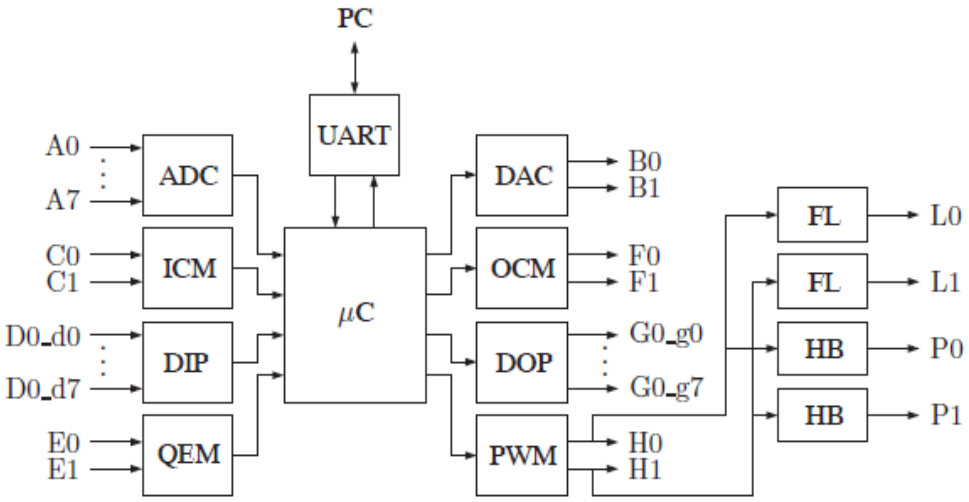


**Figure 5. 3.** Functional block diagram of the board

The real-time control board employs a DSPIC30F2012 digital signal controller for central control. The DSPIC30F2012 is a high performance 16 bit digital signal controller with 12 kB flash program memory and 1 kB SRAM data memory. The layout of the board is given in Figure 5.4.

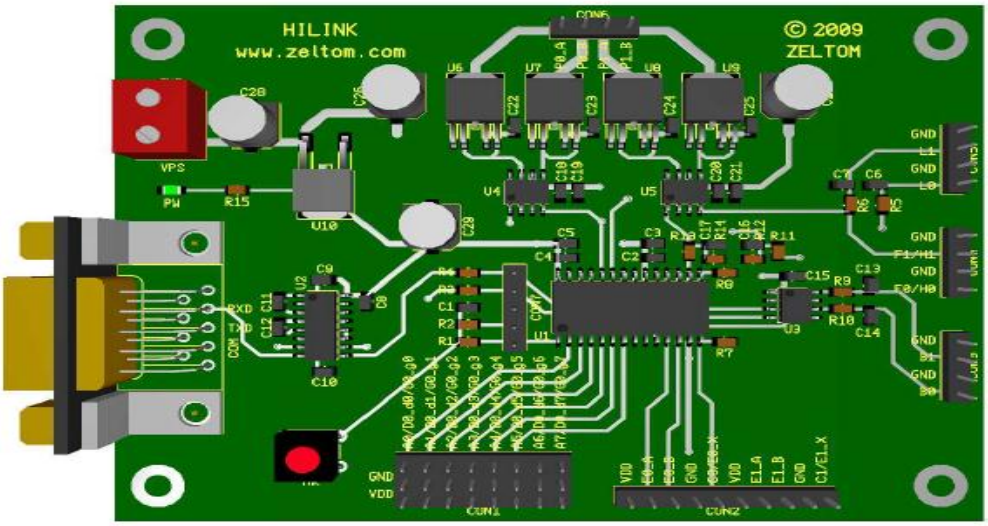


**Figure 5. 4.** Component layout of the board

### 5.6. Real-Time System Experiments

In the previous chapter state feedback controller is designed to control the simulated manipulator system. The same controller is adopted to the real prototype manipulator in Simulink environment. Thus PC serves as a data acquiring and processing system. Its main task is to deal with the measurement information and send out the calculated control signal accordingly. General hardware system is shown in Figure 5.5.

Encoder inputs, DC motor model and controller is combined in the Simulink and real-time controller unit is obtained. Physical parameters of the manipulator given in this chapter is used in the controller. Sample time of controller is chosen as 1/2048 s and total application time of controller is adjusted to 20 s. Controller used for real-time control experiment can be seen in Figure 5.6.

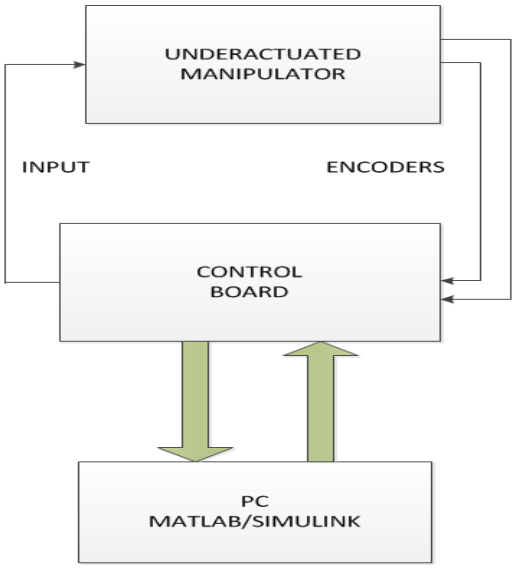


**Figure 5. 5.** Configuration of underactuated manipulator hardware system

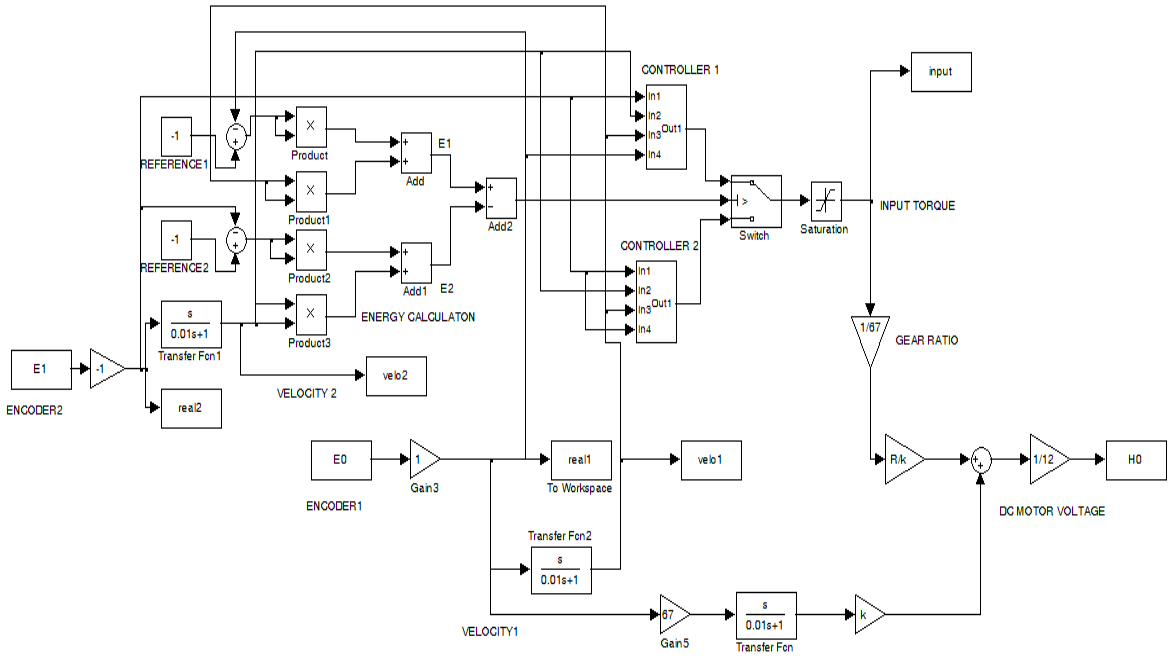


**Figure 5. 6.** Control system used in real-time application

Before giving the information about results and performance of the controller, a comparison is made between simulated system and real-time manipulator system. The obtained results are given in Figure 5.6. As we can see from this comparison results, for the same input torque, the change of joint angles of real prototype system follows joint angles of its realization in Simulink with very small errors. In fact, in this case, comparison of final position values of joint angles is more important since we do not apply  a trajectory control to the system.

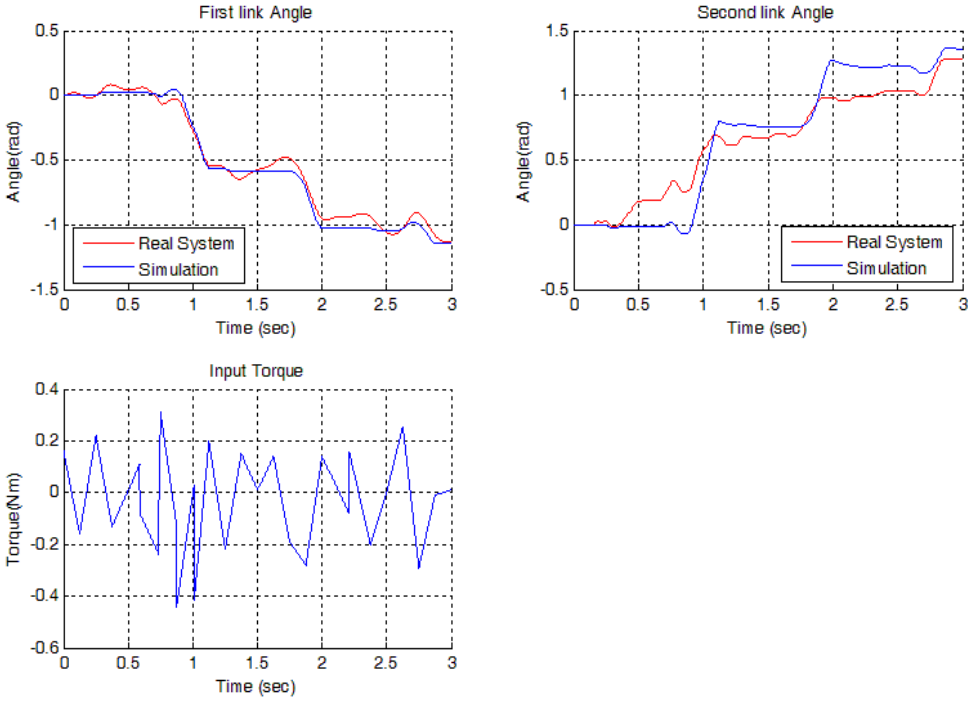


**Figure 5. 7.** Joint angle changes of simulated and real-time system for the same input torque

In the experimental results, firstly, to show controller performance three desired state vector for joint angles and velocities are chosen as given in simulation part of thesis. As pointed out before considering maximum velocities available PD control gain values are adjusted to $K_{p1}$ = 49.0, $K_{v1}$ = 14, $K_{p2}$ = 225.0, $K_{v2}$ = 30.0 which are the same with the controller applied to simulated system. Since we use incremental encoders for both joint of underactuted manipulator in real-time application, every initial angle value is always zero radian. In this case initial condition for all experiments are chosen as $x_d = [0 \quad 0 \quad 0 \quad 0]^T$. To this end, various desired state vectors are defined. To show controller performance in real-time prototype of the manipulator some desired state vectors can be given as follows :

$$x_{d1} = [2 \quad 0 \quad 0 \quad 0]^T$$

$$x_{d2} = [0 \quad 0 \quad 1.5 \quad 0]^T$$

$$x_{d3} = [1 \quad 0 \quad -1 \quad 0]^T$$

$x_{d4} = \begin{bmatrix} 1 & 0 & 1 & 0 \end{bmatrix}^T$

### 5.7. Results and Discussion

For desired condition $x_{d1} = \begin{bmatrix} 2 & 0 & 0 & 0 \end{bmatrix}^T$, Figures 5.7 - 5.9 show variations of manipulator joint angles, velocities and input torque with time. It can be seen that both joints reach desired position values quickly with small errors. Also for desired state vectors $x_{d2} = \begin{bmatrix} 0 & 0 & 1.5 & 0 \end{bmatrix}^T$, $x_{d3} = \begin{bmatrix} 1 & 0 & -1 & 0 \end{bmatrix}^T$ and $x_{d4} = \begin{bmatrix} 1 & 0 & 1 & 0 \end{bmatrix}^T$ Figure 5.10-5.12, Figure 5.13-5.15 and Figure 5.16-5.18 show these variations for each desired condition respectively.

The errors that occur in the system response can be based on some parametric uncertainty such as mass and inertia of the links, inertia values and joint frictions. This error can be decreased by changing gain parameters to some certain values.

From figures, it can seen that applied torque to the system has a non-zero value but this torque value is not enough to drive the system to the exact desired positions. Also we can see that behavior of the system changes depending on the desired state vectors such that if we try to move two joint angles to different values, amplitude of joint position values in the transient part of the joint angle responses increases and input torque activity increase such that in small time interval input torque applied to the system changes quickly.

In the end, depending on the initial configuration of the system and desired position and velocity values control effort can be hard or simple. However, it can be seen from various experiments done with different desired state values that controller is able to move joint positions to predefined values of it.

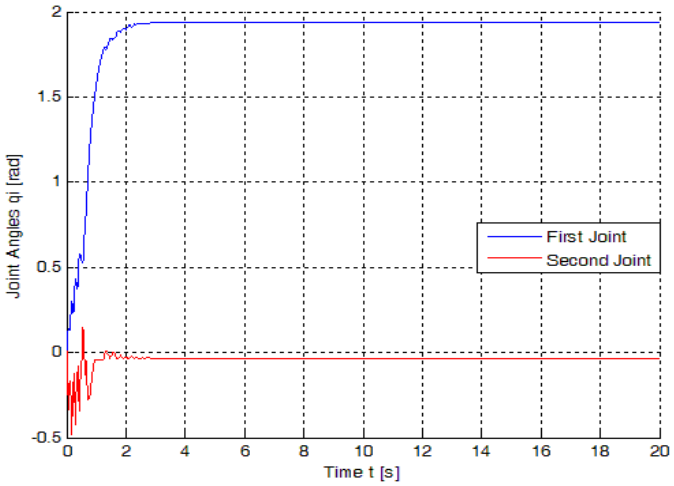


**Figure 5. 8.** Joint angles for desired state $x_{d1} = \begin{bmatrix} 2 & 0 & 0 & 0 \end{bmatrix}^T$

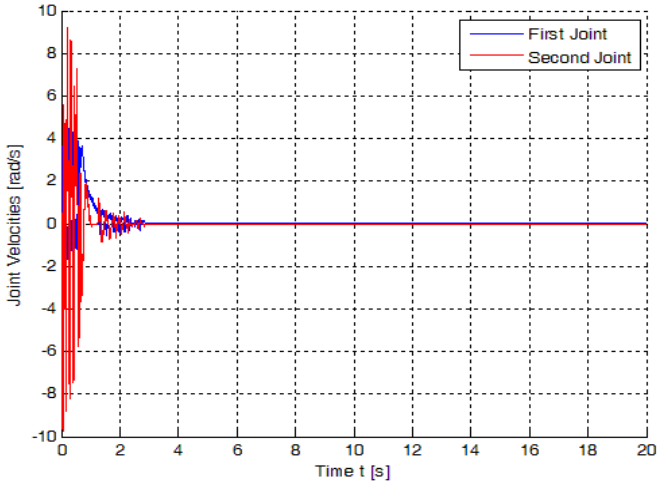


**Figure 5. 9**. Joint velocities for desired state $x_{d1} = \begin{bmatrix} 2 & 0 & 0 & 0 \end{bmatrix}^T$

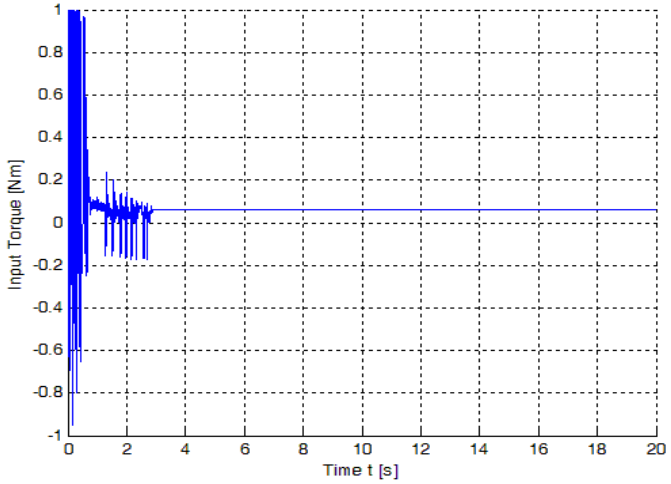


**Figure 5. 10.** Input torque for desired state $x_{d1} = \begin{bmatrix} 2 & 0 & 0 & 0 \end{bmatrix}^T$

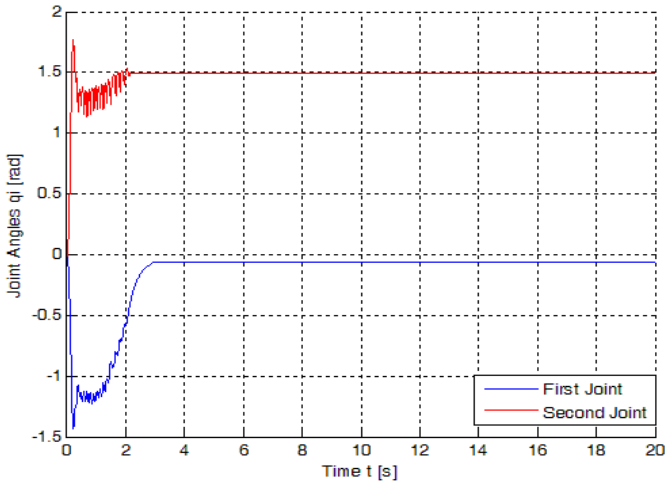


**Figure 5. 11.** Joint angles for desired state $x_{d2} = \begin{bmatrix} 0 & 0 & 1.5 & 0 \end{bmatrix}^T$

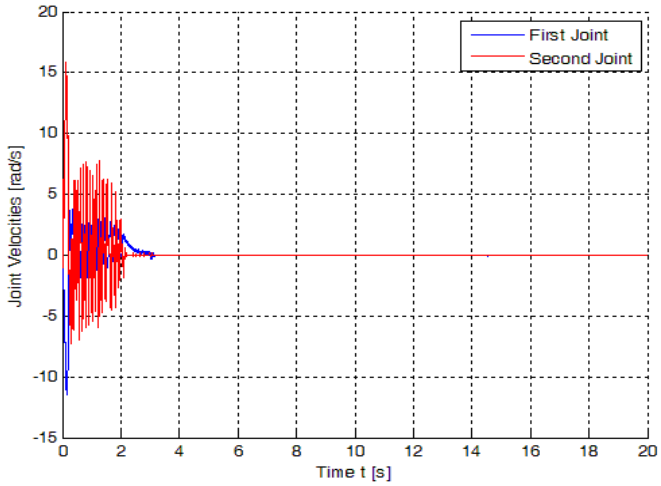


**Figure 5. 12.** Joint velocities for desired state $x_{d2} = \begin{bmatrix} 0 & 0 & 1.5 & 0 \end{bmatrix}^T$

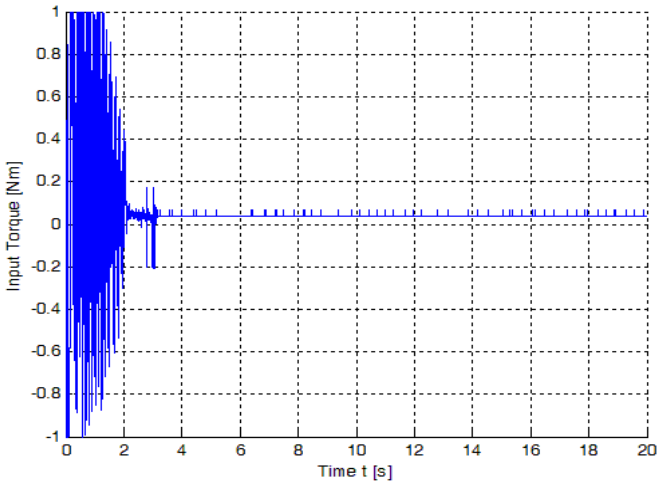


**Figure 5. 13.** Input torque for desired state $x_{d2} = \begin{bmatrix} 0 & 0 & 1.5 & 0 \end{bmatrix}^T$

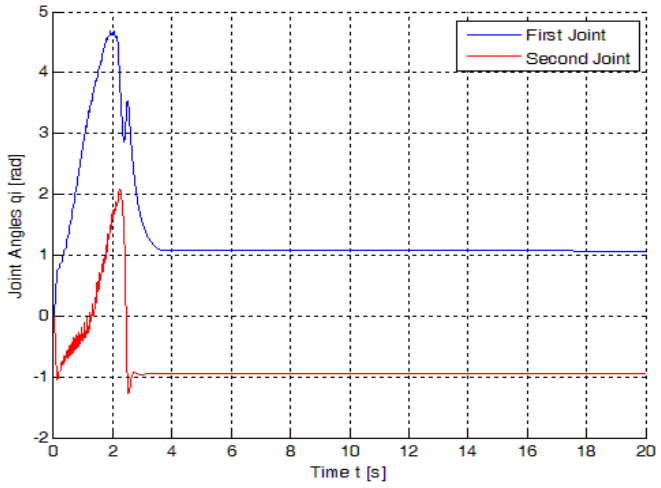


**Figure 5. 14.** Joint angels for desired state $x_{d3} = \begin{bmatrix} 1 & 0 & -1 & 0 \end{bmatrix}^T$

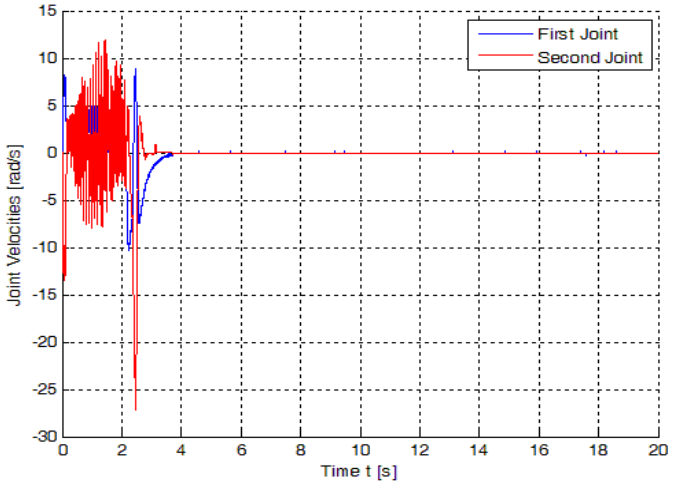


**Figure 5. 15.** Joint velocities for desired state $x_{d3} = \begin{bmatrix} 1 & 0 & -1 & 0 \end{bmatrix}^T$

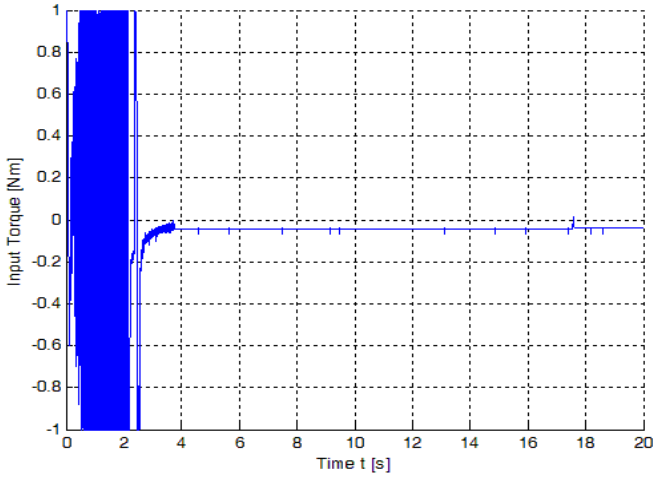


**Figure 5. 16.** Input torque for desired state $x_{d3} = \begin{bmatrix} 1 & 0 & -1 & 0 \end{bmatrix}^T$

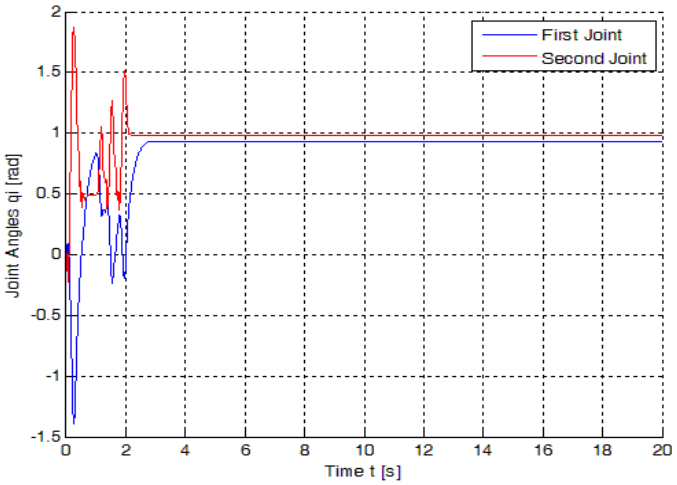


**Figure 5. 17.** Joint positions for desired state $x_{d4} = \begin{bmatrix} 1 & 0 & 1 & 0 \end{bmatrix}^T$

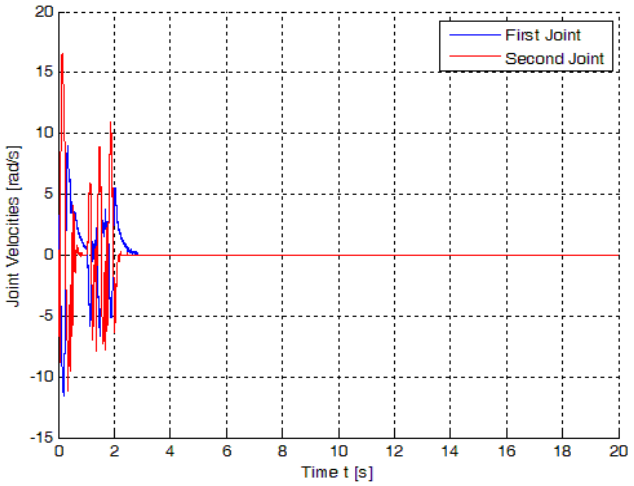


**Figure 5. 18.** Joint velocities for desired state $x_{d4} = \begin{bmatrix} 1 & 0 & 1 & 0 \end{bmatrix}^T$

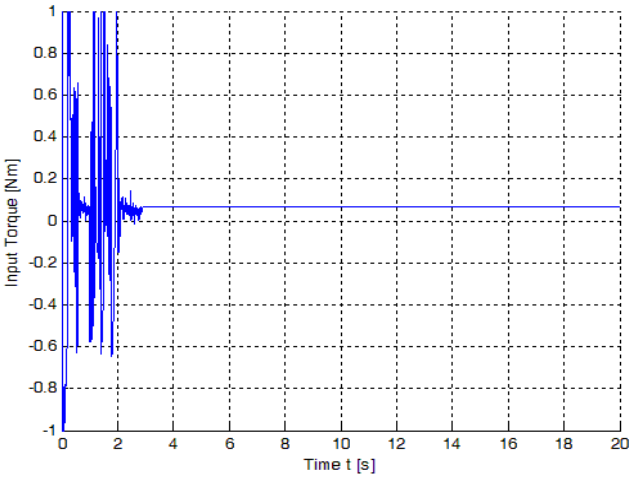


**Figure 5. 19.** Input torque for desired state $x_{d4} = \begin{bmatrix} 1 & 0 & 1 & 0 \end{bmatrix}^T$

Controller gain values are adjusted their appropriate values after some explorations as mentioned before. PD gain values of Controller 2 are chosen to be higher than those of Controller 1 since motion of Link #2 is excited by the motion of Link #1 and in this case we need faster error convergence rate for link 2 while Controller 2 is active and error of link 1 is getting higher. In the same manner, Controller 1 gain parameters are chosen to be small enough to steer link 1 to its desired position while it does not excite link 2 position. By looking at the experimental results in the relevant figures, it can be seen that the control input torque activity is very high and as a result of this link velocity can be higher. In the case of both joint error energies are very close and since Controller 2 indirectly by dynamic coupling between links and it has high gain value, controller switches rapidly and applied torque can change very fast in a short duration with high amplitute. The response given for the desired state $x_{d3}$ is an example of that. In some cases, dynamic coupling between links can be adventageous such as the controller chosen by the switching algorithm can also decrease the position error of other link. The response given for desired state $x_{d4}$ is an example of that.

Using PD controller at the outer loop control of partly stable controllers is very effective if all the manipulator parameters are known and there is no disturbance. In the presence of constant disturbances, PD control gives a nonzero steady-state error. A common modification is to add an integrator term to eliminate steady-state errors. This introduces additional complications since care must be taken to maintain stability and avoid integrator windup. It is important to be aware of an effect in implementing PID control on any actual system that can cause serious problems with integral control due to windup. PID controller in partly stable controllers can ruin critically damped response and since we use continuous and in some cases fast switching between controllers it can increase the settling time or prevent the system settling to any value and has a negative impact on small amplitude oscillations in the steady state part of position response. Figures 5.20-5.22 shows PID applied outer loop controller case system position responses. It can be clearly seen that PID controller tries to make the errors zero but overshoot behavior and fast switching prevent the system position error approaching zero.

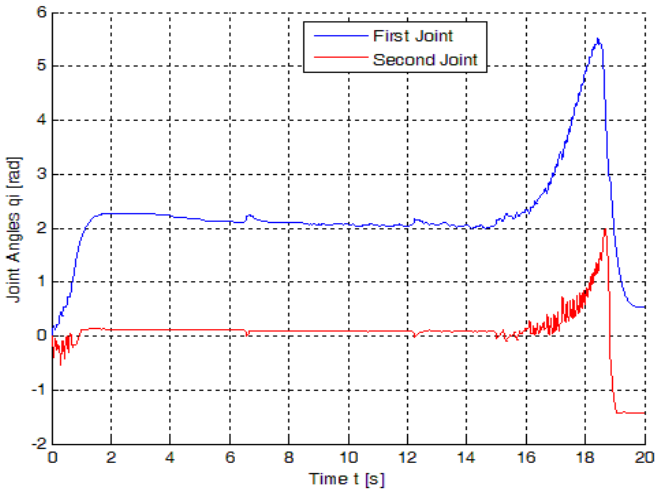


**Figure 5. 20.** Joint angle outputs of PID controlled system for desired position $x_{d1}$

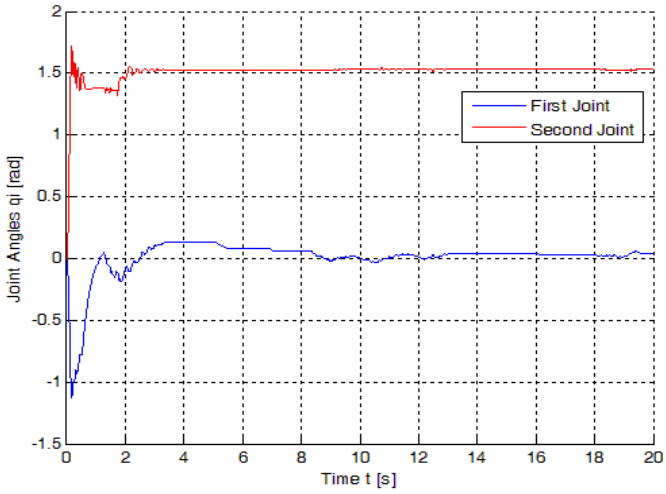


**Figure 5. 21.** Joint angle outputs of PID controlled system for desired position $x_{d2}$

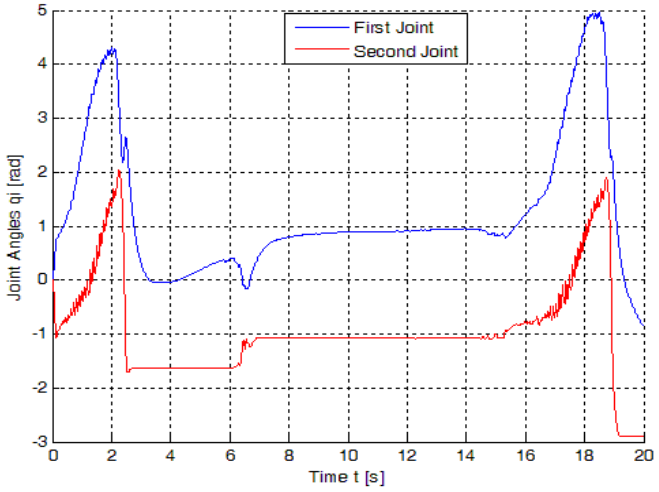


**Figure 5. 22.** Joint angle outputs of PID controlled system for desired position $x_{d3}$

# CHAPTER VI

# CONCLUSIONS

## 6.1. Concluding Remarks

The objective of this work was to develop and implement a state feedback control system for a two-link planar underactuated manipulator. Its actuated joint is located at the shoulder and the elbow joint is unactuated and allowed to rotate freely. The states of the manipulator system are comprised of the joint angular positions and joint angular velocities. Two partly stable controllers are designed for the manipulator joints. Partial feedback linearization technique is used to design their control that stabilizes each joint. Then, in order to control two links of the manipulator simultaneously, a switching control algorithm is adopted to the system. State feedback control system that is composed of partial feedback linearization technique and switching control is implemented to a simulated manipulator in Simulink and a real prototype of manipulator. Results of simulated system and real system are presented demonstrating the performance of the system with the controller in related chapters.

Firstly, controller performance is observed in simulated system and various initial state vectors are chosen and in each time, it is observed that system goes to desired positions in a short time with small position errors which are arisen from switching control. Secondly, the same controller is used in real-time prototype system. Digital encoders are used for high precision angle measurement and a control board is used sending the control signal to the manipulator and collecting data form encoders and sending them to PC which processes these data according to control algorithm and calculates control input.

As a result, purposed control system moves the manipulator links to desired position in a short time interval and input torque needed is small enough to apply the controller to a real manipulator system. Simulation results also show that we achieve position control objective with small steady-state errors. These errors occurs with

very small amplitude oscillation since we use a switching control method. Using PD control for the outer loop controller of partly stable controllers is very effective if all the arm parameters are known that in the presence of constant disturbances, PD control gives nonzero steady state error. Therefore, a PID controller is adopted also at the outer loop controller. PID controller in partly stable contollers ruins critically damped response and since we use continuous and in some cases fast switching between controllers it increase the settling time or prevent the system settling to any value and has a negative impact on small amplitude oscillations in the steady state part of position response. Also in real-time application, PID controller performance is observed and it is seen that PID control is not conveniant to use in order to decrease steady state error although in the case of disturbance this control method is required.

### 6.2. Future Work and Recommendations

In the future research, switching control algorithm can be improved so that number of switching in the transient part of position control decreases and less oscillation can occur in the transient part of response Convergence rates of position errors can also be improved. Additionally, it can be seen that steady state errors occurred in the real-time position control is higher than that of simulations, also these errors can be eliminate and if switching number in the transient part can be decreased in this case PID outer loop control can be adopted to the partly stable controllers.

## REFERENCES


[1] Block, D.J. (1996). Mechanical design and control of pendubot. University of Illinois at Urbana–Champaign.

[2] Fantoni, I. &. Lozano, R. (2002). Non-linear control for underactuated mechanical systems. London. Springer-Verlag London Limited.

[3] Giua, C. G., & Usai, A. (1998). An implicit gain-scheduling controller for cranes, *IEEE Trans. Control Syst. Technol*., **6**, 15–20.

[4] Spong, M.W., & Praly, L., (1996). Control of underactuated mechanical system using switching and saturation. National Science Foundation under graints CMS-9402229 and INT-9415757.

[5] Carroll, K. L. (1998). Control algorithms for stabilizing underactuated robots. *Journal of Robotic Systems*, **15**, 681-697.

[6] Wang, W., & Zhaoand, J. (2004). Design of a stable sliding-mode controller for a class of second- order underactuated systems. *IEE Proc.-Control Theory Appl*., **151**, 683 - 690.

[7] Arai, H., & Tachi, S. (1991, August). Position control of a manipulator with passive joints using dynamic coupling. *IEEE Transactions on Robotics and Automation*, **7**, 528-534.

[8] Arai, H. (1996). Controllability of a 3-DOF manipulator with a passive joint under a nonholonomic constraint. *Proceedings of the 1996 IEEE International Conference on Robotics and Automation*, **4**, 3707-3713

[9] Bergerman, M. (1996). Dynamics and control of underactuated manipulators. Ph.D Thesis, Dept. of Electrical and Computer Engineering Pittsburg, Pennsylvania. .

[10] Scherm N., & Heimann B. (2000). Dynamics and control of underactuated manipulation systems: a discrete-time approach. *Robotic and Autonomous Systems*, **30**, 237-248.

[11] Zhixiang T., Hongtao W., Chun F. (2010). Hierarchical adaptive backstepping sliding mode control for underactued space robot. *IEEE Automation and Robotics*, **1**, 500-503.

[12] Bortoff, S.A, (1992). Pseudolinearization using spline function with application to the acrobot, Ph.D Thesis, Dept. of Electrical and Computer Engineering Illinois at Urbana-Champaign.

[13] Mahindrakar Arun D., Rao S., Banavar R.N., (2006). Point-to-point control of a 2R planar horizontal underactuated manipulator. *Elsevier Mechanism and Machine Theory*, **41**, 838-844.

[14] Brocket R.W., (1983). Asymptotic stability and feedback stabilization. *Differential Geometric Control Theory*, **27**, 181-191.

[15] Slotine, J. J., & Li, W. (1991). Applied nonlinear control. Prentice- Hall International INC. New Jersey

[16] Spong, M.W., (1994). The control of underactuated mechanical systems, Plenary Lecture at the First International Conference on Mechatronics, Mexico City.

[17] MATLAB & SIMULINK R2011a, (2011). Getting Started Guide

[18] Spong M.W., (1992). Partial feedback linearization of underactuated mechanical systems. National Science Foundation under graints MSS-9100618 and INT-9202168.

[19] R. Kelly, V. Santibanez and A.Loria. (2005). Control of Robot Manipulators in Joint Space. Springer. UK

[20] A. De Luca, S. Ianitti, R.Mattone, G.Oriolo, (May 2003). Underactuated manipulators: control properties and techniques. *Machine Intelligence and Robotic Control*, **4**, 113-127.

[21] Kolmanovsky I., McClamroch N.H., (1995). Developments in nonholonomic control problems. *IEEE Control Systems*, **15**, 20 - 36.

[22] Oriolo G., Nakamura Y., (1991). Control of mechanical systems with second-order nonholonomic constraints: underactuated manipulators. *30th IEEE Conference on Decision and Control*, **3**, 2398 – 2403.

[23] Izumi K., Kamada Y., Ichida K., Watanabe K., (2008). A switching control of underactuated manipulators by introducing a definiton of monotonically decreasing energy. Industrial Informatics,. 6th IEEE International Conference on, 383 – 388.

[24] Ichida K., Watanabe K., Izumi K. And Uchida N., (2006). Fuzzy switching control of underactuated manipulators with approximated switching regions. IEEE International Conference on Intelligent Robots and Systems, 586 – 591.

[25] Wang G., (2003). Observer-based feedback control methods for an underactuated robot system, M.Sc. Thesis, Dept. of Engineering Science, Simon Fraser University.

[26] Abed J.Y., (2006). Comparative study of control strategies for underactuted manipulator, M.Sc. Thesis, School of Engineering, American University of Sharjah.

[27] Suzuki T., Koinuma M., Nakamura Y., (1996). Chaos and nonlinear control of a nonholonomic free-joint manipulator. *IEEE Robotics and Automation. Proceedings*, **3**, 2668 – 2675.

[28] Kelly R., Santibanez V., Loria A. (2005). Control of robot manipulators in joint space, London, Sringer-Verlag.

[29] Kim K. H., (1991). Advences in real-time computer systems, Greenwich, CT: JAU-Press.

[30] Powell J. D., Emami-Naeini A., (2006). Feedback control of dynamic systems. 5th edition. Upper Saddle River N.J: Pearson Prentice Hall.

[31] Chang Y., Chan W., Chang C., Tao C.W., (2011). Adaptive fuzzy dynamic surface control for ball and beam system. *International Journal of Fuzzy Systems*, **13**, 1-7.

[32] User manual, (2010). Real-time hardware-in-the-loop control platform for Matlab/Simulink

[33] Niku S.B., (2001). Introduction to robotics analysis, systems, applications. New Jersey : Prentice Hall.

[34] Mingjun L., Baoli M., (2010). Control of underactuated manipulators with uncertain static friction. Control and Decision Conference (CCDC), 676-679.

[35] Ratajczak A., Janiak M., (2011). Motion planning of the underactuated manipulators with friction in constrained state space. *Journal of Automation Mobile Robotics and Intelligent Systems*, **5**, 33-40.